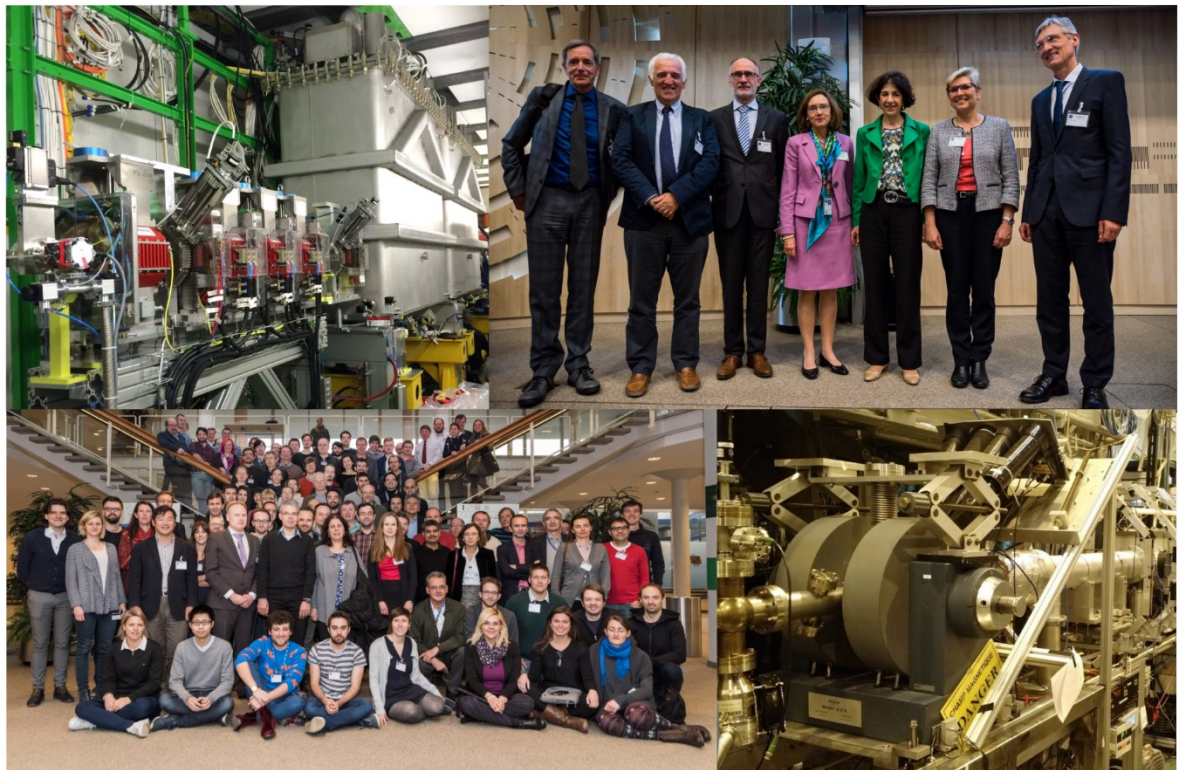


# ISOLDE

# Newsletter 2017



## In this issue

[Introduction](#)

[Information for users coming to ISOLDE in 2017](#)

[ISOLDE targets and ion sources:](#) • [RILIS status update and equipment consolidation](#) • [Target and Ion Source Development](#)

[HIE-ISOLDE project:](#) • [Beam Commissioning and Operations of REX/HIE-ISOLDE](#) • [ISS solenoidal magnet successfully recommissioned](#)

[Ground-state properties:](#) • [2016 at the Collinear Resonance Ionisation Spectroscopy \(CRIS\) experiment](#) • [First online application of the Phase-Imaging Ion-Cyclotron-Resonance technique at ISOLTRAP](#) • [Precision mass measurements of neutron-rich chromium isotopes with ISOLTRAP](#)

[Beta-decay studies:](#) • [Study of the  \$\beta\$ -delayed  \$\alpha\$  decay of  \$^{16}\text{N}\$  at the ISOLDE Decay Station](#) • [Study of octupole coupling in  \$^{207}\text{Tl}\$  at the ISOLDE Decay Station](#) • [Beta-delayed fission in  \$^{188}\text{Bi}\$  and shape-coexistence and shape-evolution studies for bismuth isotopes by in-source laser spectroscopy](#) • [Search for scalar currents in the  \$\beta\$ -delayed proton decay of  \$^{32}\text{Ar}\$](#)

[RIB applications to medical and solid-state physics:](#) •  [\$^{68\text{m}}\text{Cu}/^{68}\text{Cu}\$  as a new probe for hyperfine studies](#) • [Lattice location of  \$^{27}\text{Mg}\$  in differently doped GaN](#) • [Cd and In-doping in  \$\text{SnO}\_2\$  gas sensor by means of the TDPAC technique](#) • [A new laser polarization setup at ISOLDE](#) • [20 years of  \$^{57}\text{Mn}\$  \(1.5 min.\) for  \$^{57}\text{Fe}\$  emission Mössbauer spectroscopy](#)

[Studies with post-accelerated beams:](#) • [Reaction study of neutron rich Li isotopes](#) • [First run with IS562 using HIE-ISOLDE](#) • [Coulomb excitation of  \$^{142}\text{Xe}\$](#)  • [Statistical properties of warm nuclei: the photon strength function of  \$^{67}\text{Ni}\$](#)

[Support and contacts](#)

[isolde.web.cern.ch](http://isolde.web.cern.ch)



## Introduction

*M.J.G. Borge*

*ISOLDE leader & spokesperson*

The year 2016 will pass into the history of ISOLDE as the one where the completion of the first stage of the HIE-ISOLDE energy upgrade with two cryomodules took place. This was celebrated on the 28<sup>th</sup> of September with large participation of the different stakeholders and large representation of the CERN directorate. By then a couple of experiments were already carried out using Coulomb excitation to probe the structure of  $^{110}\text{Sn}$  and  $^{142}\text{Xe}$ . The six experiments realised with post-accelerated beams spanned from  $^9\text{Li}$  to  $^{142}\text{Xe}$  and the energies from 4 to 6.7 MeV/u the latter for  $A/q = 3$ . We were very satisfied to see the good functioning of the system.

The issue found in 2015 with the cavities's RF couplers was solved by changing the material of the coupler and improving the heat dissipation. The new coupler had already been tested in November–December 2015 and implemented into the newly built second cryomodule (CM2) that arrived at the ISOLDE hall on March 1<sup>st</sup>. The first cryomodule made its way back to the clean lab at SM18 and came to ISOLDE on the 19<sup>th</sup> of April. In between, the upgraded RF amplifier for the 9-gap was put into operation. All these novelties have kept the community in continuous excitement. In parallel, a Coulex school was organised on the 27-29<sup>th</sup> of January to prepare the young generation for Coulomb excitation experiments. By watching the intense activity dedicated to the commissioning and preparations of the linac as well as seeing the two beam lines of HIE-ISOLDE fully equipped and ready to take data we were as happy as a child with a new toy. All sparkling new, ready to deliver good physics!

A successful project should be based on a vibrant facility and that is what ISOLDE has proven to be once more over the last year. The year started with the production of a pure  $^7\text{Be}$  target for  $n_{\text{ToF}}$  to study the  $^7\text{Be}(n,p)$  reaction, one of the main destruction channel of  $^7\text{Li}$  produced from electron capture of  $^7\text{Be}$ . As the predicted amount of  $^7\text{Li}$  in the Big Bang nucleosynthesis and the one measured differ by a factor of 3, it is important to obtain a precise determination of the  $(n,p)$  cross section. This endeavour involved ISOLDE and  $n_{\text{ToF}}$  collaborating for the first time in the realisation of an experiment. Two hundred GBq of  $^7\text{Be}$  was obtained at

PSI from the water cooling of a SINF spallation source and put in an ISOLDE target container. With the help of RILIS a pure  $^7\text{Be}$  source was produced and collected at the GLM station. After this collaborative effort – which had to be repeated a second time – we started the ISOLDE program that lasted until mid-November and allowed for 47 experiments to be realised including six experiments with HIE-ISOLDE and the first polarised beams in the new beamline (more details in this Newsletter) as well as the commissioning of the second HIE-ISOLDE beam line, XT02.

The complementarity between different devices and their state of the art capabilities allows for pushing the limits of physics. This is one of the strong points of ISOLDE that facilitates its continuous success. This year the mapping of the region between  $N=40$  and  $N=50$  has dominated the scientific panorama. Subshell effects in  $N=40$  were explored by mass measurements of Cr isotopes, reaching the  $N=40$   $^{63}\text{Cr}$  with the MR-ToF. The hyperfine structure of  $n$ -rich Ni was explored with COLLAPS reaching  $N=40$   $^{70}\text{Ni}$ , however, missing  $^{69}\text{Ni}$  due to the more complex structure. The  $n$ -rich Cu isotopes were measured with CRIS almost reaching the  $N=50$  shell closure. The single particle versus collective degrees of freedom in  $^{78}\text{Zn}$  were studied by Coulomb excitation. Polarised beams in the newly designed, built and commissioned line were measured with Na beams reaching the same polarisation level as previously measured at the COLLAPS setup. An important step for M. Kowalska's beta-Drop-NMR ERC grant.

It is certainly in our interest to push for beam developments which we do in our periodic meetings of the Group of the Upgrade of ISOLDE (GUI). This group has, as part of its mandate, to identify programme-driven priorities for beam developments. At the same time, one cannot forget that sometimes the development of a new beam comes as an unexpected and nice surprise. This was the case of the Ge beams. A mass marker of sulphur was added to a  $\text{ZrO}_2$  target to check the production and release of GeS and...Bingo! a strong beam of  $^{64}\text{GeS}$  was produced dominating and hampering the  $^{68}\text{SeOC}$  production. In this way a new beam came in 2016 to be part of the large ISOLDE portfolio. The mandate of the

GUI group goes beyond beam developments to all aspects of the Facility as it can be read in: <http://isolde.web.cern.ch/gui-mandate#overlay-context=group-upgrade-isolde-gui>. This includes the new robust and reliable tape station designed to replace the existing one and placed in the hall on beam line LA2 to check its reliability and compare the results with the existing one. The present tape station will be removed definitively during the next winter shutdown after more than 40 years of operation.

The building 508, finished in 2014, is now fully functioning. It was impressive to see how extensively its rooms are used in a very dynamical way. It is clear for everyone that the DAQ room is for the experiment running at each moment. The meeting room is extensively used for presentation to visitors, experiment meetings, work and discussions. This building has become a lively place and meeting point between the users and the technical and operation personnel, exactly as planned. The only unpleasant point was the high temperatures on the first floor during the summer. I am happy to announce that a water cooled air conditioning system has been installed this winter and we hope to enjoy the fresh air to cool the discussions during our long working hours.

We witnessed an ever increasing number of visitors that exceeded 1200 in 2016. I would like to thank Kara Lynch for the extra task of coordinating all these visits. Due to safety requirements it is compulsory to send in advance the name of all visitors to Alexander Dorsival (RP).

Many of you have already profited from ENSAR2 transnational access funds. In 2016, 688 days were distributed in three meetings organised soon after each release of the schedule. I would like to thank the committee members B. Blank, K. Riisager, K. Blaum, P. Van Duppen, K. Johnston, J. Schell and myself for their availability to quickly distribute the funds once the schedule is released. Thanks to J. Weterings who facilitates enormously this task. A similar number of daily allowances will be distributed in 2017 and 2018, of which a small part will be distributed to our non European partners.

The annual ISOLDE workshop and users meeting was held at CERN on 7-9 of December 2016 with more than 140 participants. The meeting benefited from a satellite workshop organised by the ENSAR2 physics network NUSPRASEN on the 6<sup>th</sup> of December. This network aims at raising synergies between the various ENSAR-2 work packages, its transnational access facilities and their

users. This joint adventure has been a very good experience that will be repeated with other programmed meetings and annual facility meetings in the near future. The atmosphere of the ISOLDE workshop was fantastic due to the attendance, the excellent choice of invited speakers and the remarkable quality of the presentations (<https://indico.cern.ch/event/561089/>), many delivered by young researchers. The lively discussions and friendly atmosphere make the poster session, the coffee breaks and the dinner a great success. The photo on the cover taken during the workshop is a good reflection of the lively meeting. I had the privilege this time of closing the meeting and presenting the four prizes sponsored by CAEN to the best posters and best young speakers, a consolidated tradition added to our annual ISOLDE meeting. This was the last meeting I will organise as ISOLDE Group Leader and I strongly appreciated the kind words given by Yorick Blumenfeld. Organising these meetings has been a great pleasure due to the wonderful assistance and the help of fellows and students. They are the power of ISOLDE and I express to them my profound gratitude.

We continue to organise a group meeting every Wednesday at 14:00 in the visitor's room. You are all welcome to attend the meeting when you have an experiment and you are especially welcome to come and hear the latest technical news and to inform us of the physics case to be studied. The meeting is followed by a seminar and you are very welcome and encouraged to present us your research. Please contact Vladimir Manea and/or me for fixing a date. It could also happen that the meeting takes place outside CERN as it was the case for the ISOLDE outing to the Jura that took place on the 22<sup>nd</sup> of February this year and I am sure that it will not be the last. See photo.



ISOLDE outing to Le Touret on February 22<sup>nd</sup>, 2017

A new edition of the European Long Range Plan was launched by the Nuclear Physics European Collaboration Committee, NuPECC, with a large participation of our community. The first draft was ready for distribution before Christmas 2016 and the final discussion about the priorities concerning the different facilities in Europe took place in Darmstadt 11-13 of January 2017. As a result of the town meeting the priorities and recommendations were discussed in detail in the NuPECC meeting hosted by ISOLDE on March 9-10 2017. The final document will be approved by NuPECC in the next meeting in June in Lisbon and sent for printing during the summer.

On October 16, 1967, ISOLDE received its first radioactive beams according to the CERN Courier (7, 206) paving the way for 50 years of success. In order to celebrate this anniversary during 2016 we launched a special issue dedicated to ISOLDE: "Focus on exotic beams at ISOLDE: A Laboratory Portrait" that will be published in the Journal of Physics G: Nuclear and Particle Physics. It addresses the highlights since the last portrait published in Hyperfine Interactions; HFI 129 (2000). We expect to release it in June and it will contain invited and individual contributions. I would like to thank

the community for their efforts in making this new issue a success.

During 2016 we have proceeded to the renewal of the present MoU of the ISOLDE collaboration. We profited to update the annexes that now reflect both the investments in HIE-ISOLDE as well as the new instrumentation present in the experimental hall. From now on the MoU will be automatically renewed every three years. Once again thanks to Jenny Weterings for her persistence in getting the information from the different Collaboration representatives in order to have a good update of the MOU annexes.

Just before I finish I would like to take the opportunity to thank the technical and physicist teams that have made 2016 again a very successful year as witnessed by the contributions included below in this edition of the ISOLDE Newsletter. These years here have been challenging and wonderful. We have faced difficulties and enjoyed successes, my gratitude to all of you for sharing the adventure of science together. My best wishes to Gerda Neyens who will enjoy after me this wonderful place.

# Information for users coming to ISOLDE in 2017

*Karl Johnston*  
*ISOLDE physics coordinator*

## Schedule 2017

ISOLDE will have protons available for physics from April 24<sup>th</sup> till November 20<sup>th</sup>. As in previous years, the schedule for 2017 is split into two distinct periods. While the commissioning of HIE-ISOLDE with three cryomodes takes place, both GPS and HRS will serve low energy physics. This period will run from weeks 17 – 26. HIE-ISOLDE is expected to resume operation in early July. Unlike the previous two years, both low and high energy physics runs will be served from week 27, although HIE-ISOLDE physics will be prioritized as best as possible. Nonetheless, it has been observed during the past year that concentrating solely on HIE-ISOLDE physics has led to a less efficient use of the machine than is desirable. To address this, low energy physics will be accommodated as best as possible during the second part of the running period in 2017.

The ISOLDE schedule can be found at <http://isolde.web.cern.ch/isolde-schedule> and more detailed weekly schedules will be sent around a few days before the beginning of the week concerned.

## User registration for 2017

A full description of the procedure for registering at CERN is given below. Visiting teams should use the [pre-registration tool](#) (PRT) to register new users.

As for 2016: the teamleader and deputy teamleader who sends the information via PRT must have a valid CERN registration. This also applies to paper forms which have been signed at the visiting institute. If the teamleader or deputy do not have a valid registration, the users office will refuse to accept the documents.

## Access to ISOLDE: ADAMS

There has been a change in how access to ISOLDE is requested. Previously this was through EDH, but has now transferred to ADaMS (Access Distribution and Management System). The access required for ISOLDE is "ISOHALL". Once submitted it will be sent for approval to the physics coordinator.

## Safety at ISOLDE

Safety remains a priority at ISOLDE. As last year, there is a variety of safety courses both online (called SIR) and hands-on (CTA) which need to be followed by all users to gain access to ISOLDE. These are more precisely detailed in the section "How to obtain access to the ISOLDE hall".

Still in force since 2016 is the requirement to wear safety shoes and helmets within the ISOLDE hall. Spare helmets are available at the entrance. It is also mandatory to check yourself on the hand-foot monitor before leaving the ISOHALL zone. Hand foot monitors are available at both Jura and HIE-ISOLDE entrances; please use them.

Once within the ISOLDE hall you have at your disposal additional protective equipment such as gloves and contamination monitors to ensure your safety. These are located in the cupboard close to the old control room.

A variety of "expert" courses are available for those required to perform more demanding operations such as those involving cryogenics, using the crane and lasers. Please ensure that you have followed these courses before performing these tasks.

For those performing electrical work (e.g. making cables, putting up HV cages) – a 3-day CERN course needs to be followed (all local physicists have followed it). If you require more information about this, please do not hesitate to contact me.

The mechanical workshop in building 508 is fully operational. If you wish to use it a document will need to be provided which signed is by your teamleader, yourself, and our workshop supervisor, authorising you to use the selected machines in the workshop. For more information, please contact your experiment spokesperson or me.

The list of contacts for safety both for local experiments and visiting setups can be found here: <http://isolde.web.cern.ch/safety>. All visiting setups should ensure that they have had a safety inspection before their experiment starts at ISOLDE. Please allow sufficient time

for this to be done. You can contact me for more information to prepare for this.

The laboratories on the ground floor of 508 where solid state physics perform chemistry now have their own access. It is required to follow the SIR course “Chemical Safety Awareness” before requesting ISO-CHEM for 508 R-002 and ISO-EXP for 508 R-008 for the measurement area.

### **Removal and shipping of equipment from the ISOLDE hall**

All equipment which has been in the ISOLDE experimental hall requires a control by radiation protection before it can be transported elsewhere or back to home institutes. A new “buffer zone” has been installed in the ISOLDE hall (close to the SAS and the HIE-ISOLDE tunnel) which implements the CERN-wide TREC system to ensure that all controlled equipment has traceability. This is now incorporated into the EDH flow for all transport requests from the ISOLDE hall.

### **Building 508 and 275: labs, DAQ rooms and kitchen**

On the ground floor of b508, within the CERN RP controlled area, the detector laboratory is now up and running. The chemical laboratory is available for occasional chemical operations, once the appropriate access has been followed, as described above.

Upstairs in building 508 the kitchen is now fully installed comprising a fridge, cooker, microwave and dishwasher. In addition, a variety of coffee machines ranging from capsules to moka pots are available. Needless to say, this should be maintained in a good condition and it is the responsibility of experimental spokespeople to ensure that it is kept in a good state.

Users can also avail of the DAQ room to monitor their experiments outside of the controlled zone.

Building 275 has received a lot of attention in the past year. A complete refurbishment of the roof has taken place and the building has now being de-classified. The former solid state laboratory is available for installation and testing of equipment prior to installation in the ISOLDE hall. If you are interested in availing of this, please write to me with a detailed request of the infrastructural needs and the time expected.

Please contact me if you have questions concerning access and use of these labs.

The local physics team can also help you with many aspects of ISOLDE experiments, e.g. turbo and pre pumps, RP sources, chemicals, etc.

### **Visits to ISOLDE**

Visits to ISOLDE are still possible. A typical visit consists of an overview presentation in the visitors’ area in building 508 and – when possible – a tour of the ISOLDE facility itself along the pre-arranged visit path. In the event of a machine intervention or a conflict with physics which happens to be running, the tour of ISOLDE may be cancelled, and one remains in the 508 gallery area.

All visits are coordinated by Kara Lynch ([kara.marie.lynch@cern.ch](mailto:kara.marie.lynch@cern.ch)) and she should be contacted well in advance with your wishes.

### **CERN hostel booking**

A block booking of 15 rooms has been reserved at the CERN hostel for visiting experiments. However, please note that there is a very strict deadline for booking these rooms. Rooms must be reserved at least **one month** in advance. After this point, the rooms will be released. A booking form will be sent to all spokespeople once their experiment has been scheduled.

### **Publications**

Please note that ISOLDE should be mentioned in the abstract of articles related to experiments performed at the facility and, if possible, the ISOLDE team should be mentioned in the acknowledgements. Experiments which have benefitted from ENSAR2 funding at ISOLDE should also mention this in the acknowledgements of any articles which emerge and which should resemble the following: “This project has received funding from the European Union’s Horizon 2020 research and innovation programme under grant agreement No 654002”.

### **Changes to bike and car rental**

CERN continues to offer the possibility of renting bicycles – either for a defined period – or in a daily manner via the “velopass” scheme. In addition, cars are available for users in certain circumstances. The new Mobility centre has been opened in building 6167 (in the Globe car park) – replacing the previous centre which was located close to the ISOLDE offices. Further details on this and on the procedures to follow in order to rent a bike or car can be found [here](#).

# ISOLDE targets and ion sources

## RILIS status update and equipment consolidation

Website: <http://rilis.web.cern.ch/>

Bruce Marsh, on behalf of the RILIS team (EN-STI-LP)

### Operational and development highlights in 2016

In 2016 the RILIS was the required ion source for more than 75 % of the ISOLDE beams produced. This equated to 130 days of operation, 22 separate RILIS runs and ionization of 14 different chemical elements. Amongst the highlights of RILIS operation were the first isomer selected ion beams of indium, two in-source resonance ionization spectroscopy studies of bismuth isotopes (IS608) and the first application of the newly-established VADLIS ion source for radiogenic Mg beams. The extension of the range of RILIS elements continued with the development of new photo-ionization schemes for Fe, Mo, Eu [1] and Ra, and the measurement of an efficiency of 18% for the Te scheme established in 2015 [2] (see Fig. 1).

As a result, ion beams of 40 elements have now been produced at ISOLDE-RILIS [3]. On-call operation of RILIS was successful for all standard RILIS runs. This was instrumental in achieving on-time setup and reliable operation for every experiment despite the unprecedented density and complexity of the RILIS schedule.

### RILIS equipment upgrades for 2017



Fig. 2: The new RILIS laser equipment that will be in use during the 2017 on-line period.

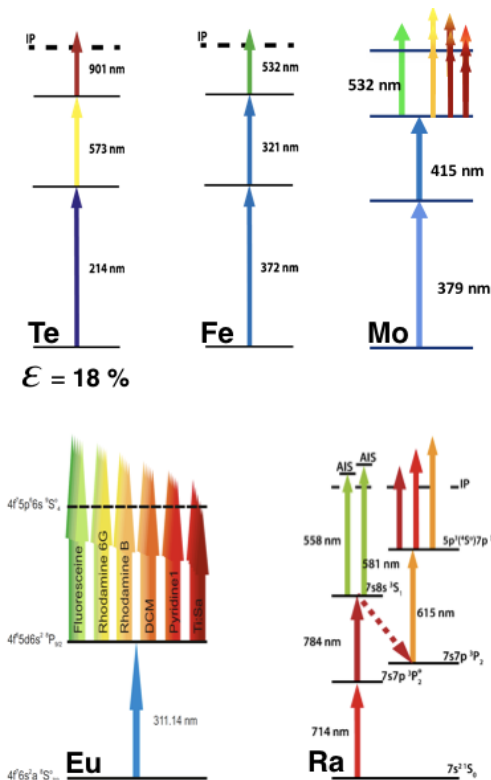


Fig. 1: Summary of RILIS ionization scheme development in 2016.

The current capabilities of the RILIS system and the feasibility of remote laser operation are a result of the use of state-of-the-art solid-state and dye laser technology, the implementation of a machine protection system designed and built by EN-STI-ECE, and the development of a comprehensive RILIS equipment monitoring and control infrastructure [4]. A RILIS equipment consolidation program has begun to ensure that our capabilities are maintained or extended in the coming years. 2017 will see the installation of a several new lasers as the first steps in a staged update of the equipment (Fig. 2):

- 2 new Z-resonator Ti:Sapphire cavities (installation ongoing in February / March)
- 1 new 40 W Coherent Blaze Nd:YVO<sub>4</sub> laser for non-resonant ionization (delivery in April)
- 1 new 100 W Edgewave Nd:YAG laser for dye laser pumping (expected in July)



This new equipment will ensure the long-term reliability of the RILIS infrastructure, whilst also improving overall the performance and ease of use of the laser systems.

[1] K. Chrysalidis et al., [Hyperfine Interact 238, 34 \(2017\)](#).

[2] T. Day Goodacre et al., [Hyperfine Interact 238, 41 \(2017\)](#).

[3] <http://riliselements.web.cern.ch/riliselements/>

[4] R. E. Rossel et al., [NIM B 317, 557-560 \(2013\)](#).

## Target and Ion Source Development

*J. Ballof, T. Day Goodacre, B. Marsh, Y. Martinez, J.P. Ramos, S. Rothe and T. Stora (for TISD and ISBM)*

Target and Ion Source Development activities have progressed in different directions in 2016; elemental  $^{64}\text{Ge}$  standing on the  $N=Z$  line of the nuclide chart was newly produced from a  $\text{ZrO}_2$  felt target, a VADIS ion source, and a Sulfur mass-marker (target #551). Secondary reactions were systematically investigated on Astatine production in thick Lead-Bismuth Eutectic targets within the LIEBE project. In the following article, we provide insights into a selection of other ongoing projects<sup>1</sup>.

### Neutron converter

The ISOLDE proton-to-neutron converter is a tungsten spallation neutron source used to produce neutrons mainly in the 1-10 MeV energy window. The produced neutrons are intercepted by a uranium carbide target producing neutron-rich fission fragment beams, while, when irradiating the uranium target directly, these beams would be contaminated with neutron-deficient isobars.

The uranium target in the current standard neutron converter design intercepts a significant amount of scattered protons from the tungsten bar (see Fig. 1a), thereby producing unwanted contaminants. Furthermore, the target intercepts a small solid angle of the emitted neutrons, which accounts for factor of about 10 lower ion beam intensities, although with higher purity, when compared to beam on target.

Following up on our previous studies [1,2], a collaboration with TRIUMF (Canada) and SCK•CEN (Belgium) was started in order to design, prototype and build an optimized neutron converter. The objective is to obtain the same ion beam intensities as with proton beam on target with much lower contaminations. In this project two versions will be developed: one for TRIUMF's 500 MeV high power proton beam (50 kW) and one for

ISOLDE taking into account the possible future 2 GeV, 6  $\mu\text{A}$  ISOLDE upgrade. One of the concepts is shown in Fig. 1b. In the conceptual development phase, FLUKA is used for neutronics and ANSYS<sup>®</sup> for thermomechanical simulations. When a concept is fixed, engineering questions will be addressed, and prototypes will be built and tested offline for validation and commissioning. Finally, it is planned to test two prototypes at TRIUMF and at ISOLDE.

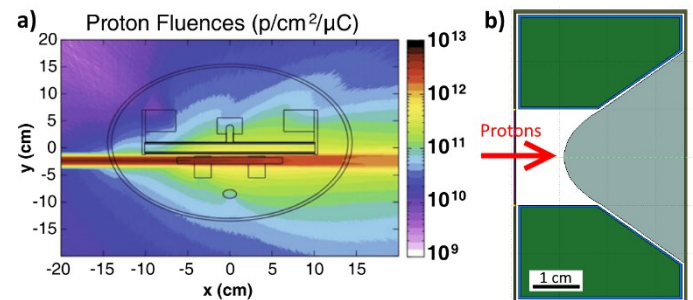


Fig. 1: (a) Proton beam scattering on the current proton to neutron converter design [1]; (b) one of the new designs under investigation where the cross-section of the uranium carbide target is shown in green, the W converter in grey and the red arrow represents the proton beam.

### The upgraded ISOLDE yield database

Developed more than 10 years ago, the ISOLDE yield database [3] still serves as a valuable source for experiment planning. At the moment, it contains in total 2445 yield entries for 1333 isotopes of 74 elements and 55 different target materials. In addition, information about the time structure of the release is available for 427 yields.

We are now restoring some of the lost features when we moved the website to Drupal<sup>™</sup> and are implementing new ones, like yield estimate for isotopes when no experimental data is available, or numerical in-target productions.

We have revised the underlying data model itself, the web application as well as the process of how new yields

<sup>1</sup> These include some activities of the Ion Source and Beam Manipulation (ISBM) working group: the development and testing of the ISOLDE negative ion source, and the further investigation of the VADIS and VADLIS ion sources.

are entered. The upgrade of the data model is finished, and a prototype web application is currently being tested, which already exceeds the functionality of the former yield database application.

### Negative ion production at ISOLDE

During the 2016 ISOLDE negative ion campaign, the negative surface ion source (MK4) was coupled to a Ta/Th foil target (#576) and beams of radioactive  $^{128}\text{I}$  and  $^{211}\text{At}$  were extracted and delivered to the laser photodetachment setup GANDALPH, located at the GLM beamline. As part of the LOI-148 [4], the first measurement of the electron affinity of a radioactive isotope ( $^{128}\text{I}$ ) was performed at ISOLDE [5]. This marks a milestone towards the measurement of the electron affinity of astatine that will enable, in combination with the previously measured first ionization potential [6], the calculation of the electronegativity of astatine.

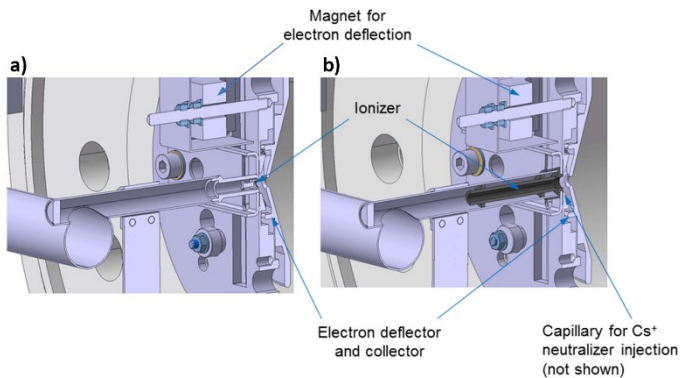


Fig. 2: Cross-section view of the target unit at ISOLDE with a negative surface ionization source with planar ionizer (a) and with a tubular ionizer (b).

To ensure reliable and efficient production of halogen beams at ISOLDE, negative ion source prototypes will be optimized and further characterized in an ongoing development campaign: a dedicated test-stand will be put in operation in 2017 enabling the study of the work-function of the source materials under extreme operation conditions. Thermal stress induced through heating cycles, and susceptibility to poisoning through addition of contaminants to the surface will be investigated. In Fig. 2, we show two types of negative ion sources available at ISOLDE to produce negative halogen beams.

### VADIS recent developments

The FEBIAD Ion Source presently used at ISOLDE for the production of radioactive beams has undergone a series of changes since it was first introduced by Kirchner in 1976 [7]. These changes were necessary not just to gain in beam intensities but also to improve the source's

reliability and stability under long periods of operation. The ionization in this ion source takes place in the anode volume by electron impact as the main mechanism. Early designs used a tantalum or tungsten filament that, when heated, emitted electrons that were accelerated towards the anode volume by biasing its walls with a positive potential. Eventually, this filament was substituted by a more robust cathode as detailed in [8] and the emitting surface became a 12 mm diameter disc resistively heated above 2000 °C for thermionic emission.

A series of both experimental and theoretical studies gave a better understanding of the different processes affecting the ionization [9]. In the case of the MK7 ISOLDE ion source, this led to the modification of the anode geometry which is better suited for the extraction of the ions. For both the MK5 and MK7 subtypes, the efficiency for noble gas ionization was also improved by reducing impurities coming from different components (e.g. the anode grid) through changing their material from graphite to molybdenum. These modifications gave birth to the VADIS (VD) series. Nevertheless, it has been suggested that molecular impurities in the range of some  $\mu\text{A}$  of  $\text{CO}^+$  or  $\text{N}_2^+$  could actually improve the ionization efficiency [10]. A set-up is under development at the ISOLDE off-line separator to study this effect in detail.

### a) Ongoing characterization and developments of the VADIS ion source with VSim<sup>®</sup> software

The CPO<sup>®</sup> software [11] was used in the past to map the internal field distribution by superimposing the electrical fields generated by the source electrodes and charges (electrons and ions), but no dynamical processes were studied [9].

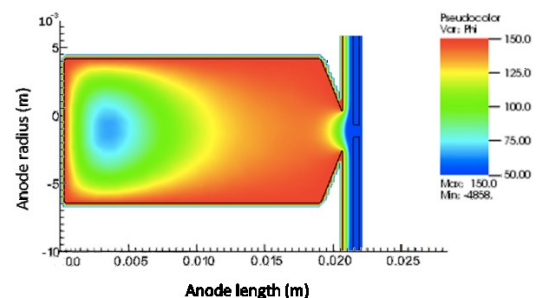


Fig. 3: Electrical field distribution inside the VADIS (simulated using VSim<sup>®</sup> software).

The VSim<sup>®</sup> software from Tech-X Corporation [12] is now used to model the low density plasma formed inside the VADIS in a more realistic way. The electrons are emitted from the cathode at each time step, with a density matching the experimentally known electron current and

are accelerated towards the anode at 150 V, producing primary ionization along their path.

Figure 3 shows the simulated electric field distribution once the electron spatial distribution equilibrium has been reached. The ions created during the ionization process are treated separately in order to reduce computation time (the mass of the electron is 4 orders of magnitude smaller than that of the ion,  $\text{Ar}^+$  in this case, and as a result their trajectories follow totally different time scales). This procedure is further justified by the fact that the generated ion current is 3 orders of magnitude lower than the electron emission current from the cathode.

A similar spatial potential distribution was already observed in ref [9]. The thermalized ions that are produced in this low-field region will be trapped, possibly decreasing the efficiency of the ion source. We are carrying out a series of simulations to investigate a means of reducing the volume of this electrical potential through the use of an optimized ion source geometry and electrical configuration.

#### b) VADLIS ion source with adjustable extraction voltage

The Resonance Ionization Laser Ion Source (RILIS) has been combined with the VADIS ion source at ISOLDE. The combination, termed as Versatile Arc Discharge and Laser Ion Source (VADLIS) has been successfully tested off-line with gallium, molybdenum and barium as well as on-line with mercury, cadmium, tin and magnesium isotopes. More details can be found in [13].

We can study the field distribution inside the VADIS cavity by using VSim<sup>®</sup> when the voltage applied to the anode walls is low, e.g. 5 V. In this mode of operation (so-called RILIS mode) there is no electron impact ionization and just laser and surface ionized ions will be created. However, the field configuration does not look optimal for efficient and fast extraction (Fig. 4 left). A modification of the ionizing cavity with an adjustable extraction electrode potential allows the application of a negative potential to the plates at the extraction side of the source. The simulations show the resulting alteration of the electrical potential map inside the anode volume. This leads to a reduction of the size of the region from which ions are not extracted. We will experimentally investigate if this modification will increase the efficiency,

and also reduce the ion extraction time as expected (Fig. 4 right).

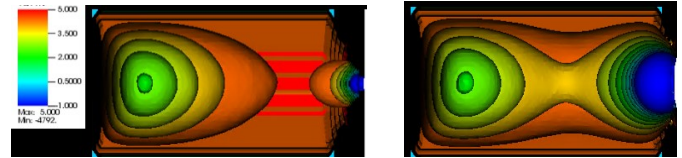


Fig.4: Electrical field lines distribution inside VADIS cavity. Anode walls are at 5V (RILIS mode). Extraction plate grounded (left) and at -150 V (right).

#### c) Efficiency measurement of metals

Beams of metal ions are essential for the physics programme at ISOLDE, for instance for nuclear structure or solid state physics studies. Due to their ionization potential, many metals are not efficiently surface ionized and we rely instead on resonance laser ionization with RILIS or on electron impact ionization with VADIS sources. While in-depth studies have been performed for the ionization of gases in VADIS sources, little information is available on the ionization efficiency of metals or other non-volatile species.

These efficiency measurements will enable a comparison with other figures reported previously for FEBIAD sources. For this purpose, a series of measurements is being performed. So far, VADIS efficiencies for manganese, mercury, gallium, tin and magnesium have been measured with values spanning from 2% to 14% in the 2035-2075 °C temperature range. A publication with more details is in preparation.

- [1] R. Luis et al., [EPJ A 48, 90 \(2012\)](#).
- [2] A. Gottberg et al., [NIM B 336, 143 \(2014\)](#).
- [3] M. Turrión et al., [NIM B 266, 4674 \(2008\)](#).
- [4] S. Rothe et al., ISOLDE LOI-I-148 (2013).
- [5] S. Rothe et al., J. Phys. G, submitted.
- [6] S. Rothe et al., [Nat. Commun. 4, 1835 \(2013\)](#).
- [7] R. Kirchner and E. Roeckl, [NIM 139, 291\(1976\)](#).
- [8] S. Sundell and H. E. Ravn, [NIM B 70, 160 \(1992\)](#).
- [9] L. Penescu et al., [Rev. Sci. Instr. 81, 02A906 \(2010\)](#).
- [10] U. Köster, PhD Thesis (2000).
- [11] CPO<sup>®</sup> [www.electronoptics.com](http://www.electronoptics.com), accessed Mar 2017.
- [12] VSim<sup>®</sup> <https://www.txcorp.com>, accessed Mar 2017.
- [13] T. Day Goodacre et al., [NIM B 376, 39 \(2016\)](#).

# HIE-ISOLDE project

## Beam Commissioning and Operations of REX/HIE-ISOLDE

Jose Alberto Rodriguez

(on behalf of BE-OP-ISO and the HIE-ISOLDE project)

The beam commissioning of REX and the first diagnostics box of HIE-ISOLDE started on wk. 26 and was done in parallel to the hardware commissioning of the two cryomodules [1]. As in 2015 [2], beam produced in the charge breeder was accelerated using the RFQ and drifted down to the HIE-ISOLDE diagnostics box. After commissioning the silicon detector in that box, the RF structures were powered-up and phased one by one.

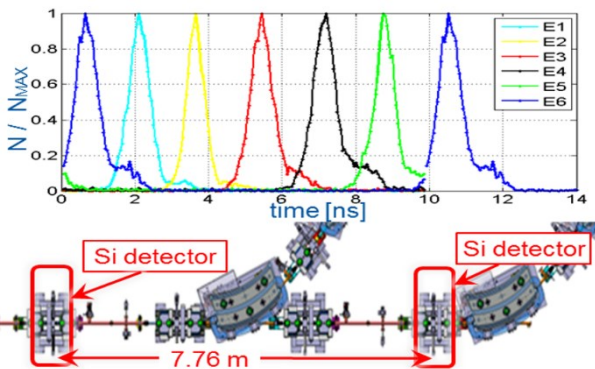


Fig. 1: Bunch structure of beam with six different energies ( $dE \approx 60$  keV/u). Changes in the TOF to the detectors were measured

The pilot beam was injected into the first cryomodule and transported to the end of XT01 on wk. 32. After testing the devices in each of the diagnostic boxes, the cavities of the two cryomodules were phased and the beam was accelerated to 5.5 MeV/u. Among others and in addition to measurements similar to those conducted the previous year [3], a new Time-Of-Flight (TOF) was tested (Fig. 1), the linearity of the silicon detectors was characterized (Fig. 2), systematic beam transmission and beam profile measurements were conducted and the impact on the beam of slow drifts in the RF settings was studied.

The high-energy Physics campaign started on Sep. 2<sup>nd</sup> when the first stable beam was delivered to the users. A week later,  $^{110}\text{Sn}$  RIB was produced in the GPS target, charge-bred to  $^{110}\text{Sn}^{26+}$ , accelerated to 4.5 MeV/u and transported to the Miniball Spectrometer. The Physics campaign continued until Nov. 21<sup>st</sup> when REX/HIE-

ISOLDE was stopped for the winter technical stop. During these twelve weeks, six different RIBs as light as  $^9\text{Li}$  and as heavy as  $^{142}\text{Xe}$  with energies between 4.3 and 6.7 MeV/u were delivered to Miniball or to the Scattering Chamber (Table 1). In addition, three stable beams were provided to test and calibrate different systems in the experimental stations. In total, approximately 685 hours of RIBs and 152 hours of stable beams were delivered to the users during the 2016 campaign.

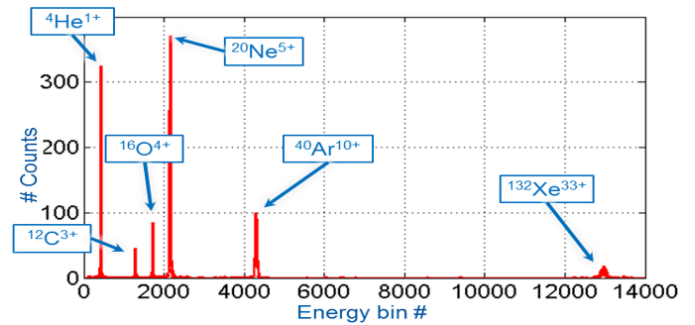


Fig. 2: Linearity on mass of a silicon detector. Response of the detector to a cocktail of ions with  $A/q = 4.0$

The main source of downtime was caused by the failure of the 9gap RF amplifier. Other issues included a leak in the laser window of the GPS separator, target failures passed their expected lifetime, problems in Linac2 and short but frequent trips of different RF structures.

Table 1: Beams provided during the high-energy Physics campaign

Exp.	Beam	Origin / Destination	$E$ [MeV/u] $\pm$ $\Delta E_{\text{HWHM}} / E$	Hours
IS562	$^{110}\text{Sn}^{26+}$	GPS / XT01	$\sim 4.5$	115
IS548	$^{142}\text{Xe}^{33+}$	HRS / XT01	$\sim 4.5$	100
IS557	$^{78}\text{Zn}^{20+}$	GPS / XT01	$4.27 \pm 0.3 \%$	130
IS551	$^{132}\text{Sn}^{31+}$	HRS / XT01	$5.49 \pm 0.4 \%$	130
IS561	$^9\text{Li}^{3+}$	GPS / XT02	$6.72 \pm 0.5 \%$	70
IS559	$^{66}\text{Ni}^{16+}$	GPS / XT01	$4.47 \pm 0.2 \%$	140
	$^{22}\text{Ne}^{7+}$	EBIS / XT01	$\sim 2.8$	60
	$^{12}\text{C}^{4+}$	EBIS / XT02	$6.72 \pm 0.5 \%$	7
	$^{132}\text{Xe}^{32+}$	GPS / XT01	$\sim 4.5$	85

Overall and despite of these problems, the campaign is

widely seen as a success both inside and outside CERN. Large amount of data was produced and relevant scientific results will likely emerge once the data is analysed.

[1] W. Venturini et al., “HIE-ISOLDE SC Linac Progress and Commissioning in 2016”, LINAC’16.

[2] J.A. Rodriguez et al., “Beam Commissioning of the HIE-ISOLDE Post-Accelerator”, IPAC’16.

[3] J.A. Rodriguez et al., “First Operational Experience of HIE-ISOLDE”, IPAC’16.

## ISS solenoidal magnet successfully recommissioned

Website: <http://npg.dl.ac.uk/isol-srs/index.html>

*Robert Page  
(for the ISS collaboration)*

The ISOLDE Solenoidal Spectrometer (ISS) project achieved a crucial milestone in February with the recommissioning of its 4T ex-MRI magnet (see Fig. 1). The magnet started its journey from Brisbane (Australia) a year ago and since arriving at CERN it has undergone an extensive programme of preparatory work. The cooling procedure finally got underway in January, supported by CERN’s cryogenics experts. The magnet was allowed to settle at liquid helium temperatures for a few days before it was “energised.”



Fig. 1: Photograph of the ISS magnet during the energising procedure at CERN in February.

The magnetic field was ramped up to the target field of 2.75T and held at this value for an hour before being ramped down again. This field is more than sufficient for the experiments already approved by the INTC that constitute an early implementation phase. These

experiments will use the original silicon detector array from HELIOS at Argonne inside the ISS magnet prior to the completion of the advanced ISS detection system.

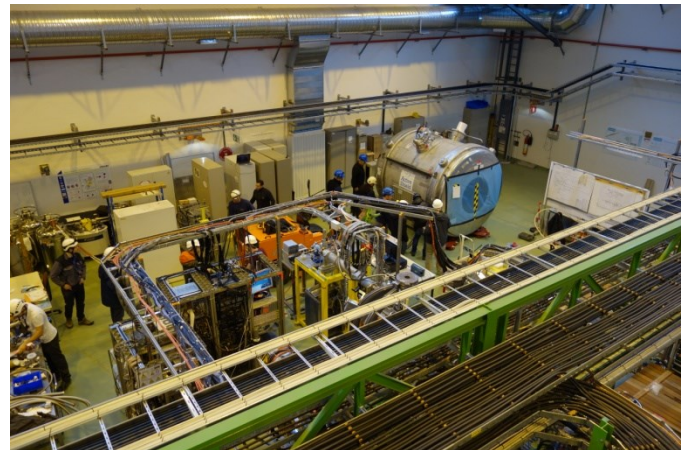


Fig. 2: Photograph of the ISS magnet being positioned inside the ISOLDE Hall in March.

The magnet was subsequently moved into the ISOLDE Hall in early March (see Fig. 2) ready for its installation on the second HIE-ISOLDE beam line (XT02). The ISS project team is also making excellent progress on the mechanical infrastructure, the detectors and the readout system. It recently took delivery of the first batch of silicon detectors and these are currently undergoing acceptance tests. The completed ISS should be available for physics exploitation after the second long shutdown (LS2). Work is also progressing well on the active target SpecMAT that will be used in separate experiments inside the ISS magnet. A physics workshop open to anyone interested in using the ISS is being planned and an announcement will be circulated shortly.

The ISS collaboration would like to thank everyone at ISOLDE and the many technical experts elsewhere at CERN for their invaluable contributions to the successful recommissioning and transportation of the magnet, and for their ongoing support of the ISS.

# Ground-state properties

## 2016 at the Collinear Resonance Ionisation Spectroscopy (CRIS) experiment

Results of experiments IS531 and IS594

Website: <http://isolde-cris.web.cern.ch/isolde-cris/>

*Agi Koszorus and Adam Vernon  
(for the CRIS collaboration)*

In 2016, two successful experiments were performed with the CRIS experiment. In April, the hyperfine structures of the ground states of  $^{63-66,68-78}\text{Cu}$  were measured together with 2 isomeric states in both  $^{68}\text{Cu}$  and  $^{70}\text{Cu}$ . High resolution coupled to high efficiency led us to resolve the hyperfine structures of  $^{78}\text{Cu}$  with about 20 ions/s production yield and a resonance linewidth of 70 MHz. (Fig. 1) [1]. In August the neutron-rich Ra isotopes were studied. The hyperfine structures of  $^{226-232}\text{Ra}$  were obtained with high resolution together with low resolution measurements on  $^{233}\text{Ra}$ . The analysis of both experiments will allow for the extraction of ground state spins, magnetic dipole moments, electric quadrupole moments and changes in mean-squared charge radii.

Improvements to the beam line and laser systems over the past year have made these measurements possible, as detailed in recent technical publications [2, 3]. A combined decay and laser spectroscopy paper of the isotope  $^{214}\text{Fr}$  was also published [4] this year, along with a technical article on the upgraded Decay Spectroscopy Station [5].

Recently two pulsed Ti:Sa lasers have been installed to replace the cavities on loan from the Johannes Gutenberg University Mainz. Furthermore, first steps towards better long-term frequency stabilization were taken and improved measurement accuracy was achieved. The newly installed DLC pro 780 diode laser together with the saturation spectroscopy module and the locking electronics will allow us to improve the accuracy of wavelength measurements, which was previously limited to 3 MHz. By locking the diode laser to one of the hyperfine transitions in Rb or K, a stable frequency reference can be obtained, which can be used for regular and reliable wavemeter calibrations. The system is completed with a Fabry-Pérot interferometer which enables us to compare the wavelength of the scanning laser to the stable frequency reference. The goal is to

reach a long term frequency stability of less than 1MHz, which will allow us to study lighter atomic systems.

Even more recently a three-axis adjustable charge exchange cell and new vacuum chamber have been installed (Fig. 2) which should increase neutralization efficiency by allowing different alkali metals to be used, at higher temperatures. In addition, a new differential pumping iris was installed, which will reduce collisional background events caused by isobaric contaminants and further enhance the sensitivity of CRIS.

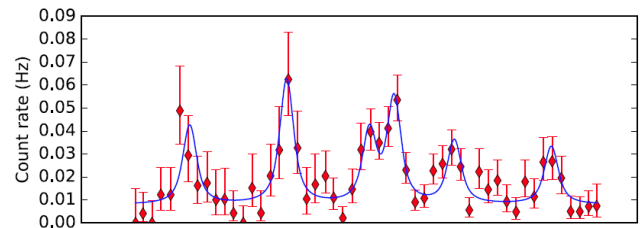


Fig. 1: Hyperfine spectra of  $^{78}\text{Cu}$  obtained during IS531. Horizontal axis is frequency (MHz) with a range of 2 GHz.

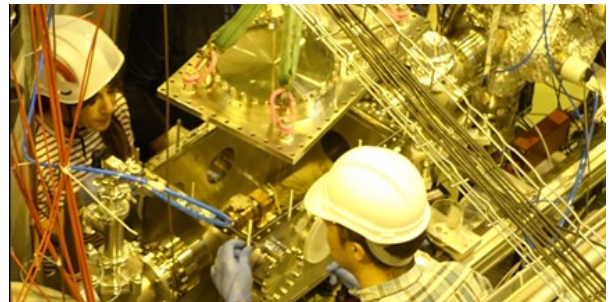


Fig. 2: The new charge-exchange cell and vacuum chamber in place at CRIS being wire sealed.

In preparation for planned experiments on In, K and Sn this year a new versatile ion source setup was installed over the summer which allows for surface ionization, plasma ionization and laser ionization of a gas stream or solid target. A new high-voltage cage arrangement around the ion source will allow extraction voltages of up to 30 kV to replicate typical beam energies from ISOLDE. This will enable us to accurately test laser ionization schemes and the neutralization efficiency of a wide variety of elements offline.

- [1] R. P. de Groote, in preparation.  
 [2] T.E. Cocolios et al. [NIM. B 376, 284 \(2016\)](#).  
 [3] R. P. de Groote, K. M. Lynch and S. G. Wilkins, [Hyperfine Interact. 238, 5 \(2017\)](#).

- [4] G. J. Farooq-Smith et al., [PRC 94, 054305 \(2016\)](#).  
 [4] K. M. Lynch et al., [NIM A 844, 14 \(2017\)](#).

## First online application of the Phase-Imaging Ion-Cyclotron-Resonance technique at ISOLTRAP

Results of experiment IS574  
<https://isoltrap.web.cern.ch>

*Andree Welker, Jonas Karthein  
 (for the ISOLTRAP collaboration)*

For more than three decades the field of Penning-trap mass spectrometry has been continuously enhanced by developing novel techniques to increase the resolution, precision and to reduce measurement time, for the study of even shorter-lived radioactive nuclides. A recent milestone was the introduction of the phase-imaging ion-cyclotron resonance technique (PI-ICR), developed by the Max-Planck-Institute for Nuclear Physics in Heidelberg [1] and later extended and applied at the SHIPTRAP facility at GSI Darmstadt [2], and used, among others, for high-precision Q-value measurements for neutrino physics [3]. This technique has now been implemented and is currently being commissioned at ISOLTRAP.

The mass-to-charge ratio  $m/q$  of an ion is determined by measuring its cyclotron frequency  $\nu_c$  in the magnetic field of the Penning trap,  $m/q = B / (2 * \pi * \nu_c)$ . In the traditional time-of-flight ion-cyclotron-resonance (ToF-ICR) technique [4], this is achieved by studying the gain in motional energy of the ions as a function of an external radio-frequency-excitation around the expected cyclotron frequency. It involves performing a frequency scan, recording the ion flight time, which depends on the energy of the cyclotron motion, between the Penning trap and a microchannel plate (MCP) detector placed about 1 m upstream. The minimal data set must include at least several tens of detected ions over the whole scan range. In contrast to the standardized ToF-ICR technique, for PI-ICR MS the frequencies of the ion motion are determined by measuring, on a position-sensitive MCP detector [5], the angle  $\Phi$  accumulated in a given period of time  $t_{\text{accu}}$  by the ion orbit in the trap. The magnetic-field gradient between the ion trap and the position-sensitive detector acts as magnification lens of the ion motion, the circular trajectory of about 0.5 mm radius described by the ions in the trap being projected in the detector plane onto a circle of up to 20 times the size.

The PI-ICR method no longer includes a frequency scan, therefore, a small number of detected ion events is already sufficient to determine the ion's mass. The SHIPTRAP studies showed that a 40-fold gain in resolving power, compared to the standard ToF-ICR technique, is achievable, as well as an up to 10 times shorter time, for the same precision. The first online mass measurement at ISOLTRAP illustrated the remarkable resolving power, of  $R = 10^5 - 10^6$ , with this novel technique. It allowed us to separate the  $11/2^-$  isomers in the neutron-rich cadmium isotopes from the corresponding ground states, as shown in Fig. 1 for the case of  $^{127}\text{Cd}$ .

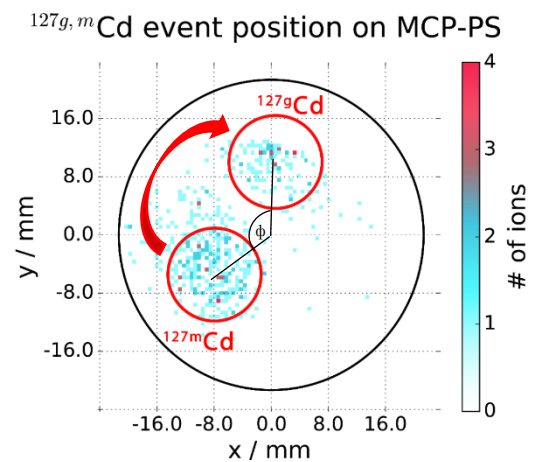


Fig. 1: The phase-imaging ion-cyclotron-resonance of the isomeric and ground state of  $^{127g,m}\text{Cd}$ . A complete phase separation was achieved with an accumulation time of  $t_{\text{accu}} = 150$  ms.

The  $^{127}\text{Cd}$  ions were excited on a circular motion around the Penning-trap center at their modified cyclotron frequency. The slight difference in their masses leads, after a certain phase accumulation time, to the well-separated images on the position-sensitive detector.

Since the end of the 2016 measurement campaign, several developments have been performed: To increase the precision, a new timing control scheme was implemented. To improve the resolving power and to reduce the distortions in the phase imaging (as the ones

observed in Fig.1), the position-sensitive detector was moved closer to the Penning trap. In addition a new event reconstruction algorithm was developed.

Further PI-ICR measurements of both short-lived isomers and beta-decay Q-values are planned for the 2017 measurement campaign at the ISOLTRAP experiment.

## Precision mass measurements of neutron-rich chromium isotopes with ISOLTRAP

Results of experiment IS532

Website : <http://isoltrap.web.cern.ch/isoltrap/>

Maxime Mougeot

(for the ISOLTRAP collaboration)

Since it was first hinted at experimentally [1] the second “Island of Inversion,” near  $N=40$ , has attracted tremendous interest from both experimentalists and theoreticians. In this region, neutron-rich chromium isotopes play a particularly interesting role due to  $Z=24$  being exactly mid-shell. However, the chromium masses were not known to a sufficient precision to reveal effects on the mass surface approaching  $^{64}\text{Cr}$ , where a maximal quadrupole deformation is thought to be reached.

Chromium is not generally considered a thick target ISOL element. However, previous experiments at ISOLTRAP using UCx targets revealed the presence of  $^{56-57}\text{Cr}$  [2]. Encouraged by this observation, a laser-ionization scheme was eventually developed [3] to enhance the yields and ISOLTRAP was able to perform mass measurements of neutron-rich  $^{59-63}\text{Cr}$  during an experiment in April 2016 (see Table 1).

isotope	Half life (ms)	Yield (ions/s)
$^{59}\text{Cr}$	1050	3E5
$^{60}\text{Cr}$	490	2E4
$^{61}\text{Cr}$	243	2E3
$^{62}\text{Cr}$	206	3E2
$^{63}\text{Cr}$	129	30

Tab. 1: Measured yields of  $^{59-63}\text{Cr}$  and corresponding half-life from literature [NUBASE 2012], for an average proton current of 1.8  $\mu\text{A}$ .

The production yields were sufficient to perform the measurement of  $^{52-62}\text{Cr}$  using the precision Penning trap. The low yield of  $^{63}\text{Cr}$  limited the measurements to ISOLTRAP’s Multi-Reflection Time-of-Flight mass spectrometer (MR-ToF-MS) [4]. Figure 1 shows a typical time-of-flight spectrum. Despite the high RILIS ionization efficiency, stable surface-ionized contaminations dominate the ISOLDE ion beam. Here again, the MR-ToF

- [1] G. Eitel et al., [NIM A, 606, 475 \(2009\)](#).
- [2] S. Eliseev et al., [PRL, 110, 082501 \(2013\)](#).
- [3] S. Eliseev et al., [PRL 115, 062501 \(2015\)](#).
- [4] G. Bollen et al., [J. Appl. Phys. 68, 4355 \(1990\)](#).
- [5] O. Jagutzki et al., [NIM A, 477, 244 \(2002\)](#).

is invaluable for its high resolving power and separation capacity.

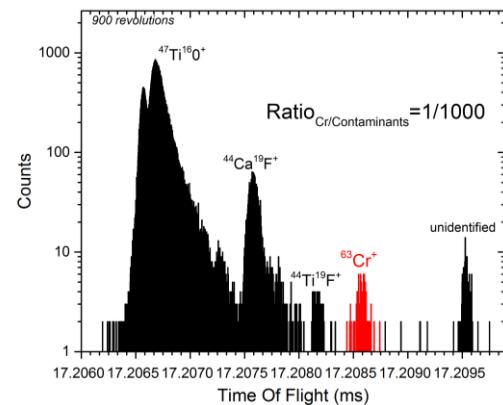


Fig. 1: MR-ToF-MS time-of-flight spectrum showing  $^{63}\text{Cr}$ , the isobaric contaminants  $^{44}\text{Ca}^{19}\text{F}$  and  $^{44}\text{Ti}^{19}\text{F}$  as well as a highly abundant  $^{47}\text{Ti}^{16}\text{O}$  peak (signal saturated).

The mass values obtained are of greatly refined precision thus shining new light on the development of ground-state collectivity towards  $N=40$  in the chromium chain. Qualitatively, the trend of the two-neutron-separation energy, derived from the ISOLTRAP measurements, hints at a much smoother development of ground-state collectivity than that inferred from previous works [5]. A more quantitative comparison to state-of-the-art theoretical predictions, including recent work on ab-initio shell-model calculations [6], is in progress.

- [1] J. Ljungvall et al., [PRC 81, 061301\(R\) \(2010\)](#).
- [2] C. Guénaut et al., [J. Phys. G 31, S1765 \(2005\)](#).
- [3] T. Day Goodacre et al., [Spectrochim. Acta, Part B 129, 58 \(2017\)](#).
- [4] R. N. Wolf et al. [IJMS 349-350, 123 \(2013\)](#).
- [5] M. Wang et al., [Chinese Phys. C 36, 1603 \(2012\)](#).
- [6] R. Stroberg et al., [PRL 118, 032502 \(2017\)](#).



# Beta-decay studies

## Study of the $\beta$ -delayed $\alpha$ decay of $^{16}\text{N}$ at the ISOLDE Decay Station

Results of experiment IS605

Website: <http://isolde-ids.web.cern.ch/isolde-ids/>

Oliver Kirsebom

(for the IDS collaboration)

While the  $^{12}\text{C}(\alpha,\gamma)^{16}\text{O}$  reaction plays a central role in nuclear astrophysics, the cross section is too small at the energies relevant to stellar helium burning to be directly measured in the laboratory. The  $\beta$ -delayed  $\alpha$  spectrum of  $^{16}\text{N}$  can be used to constrain the astrophysical S-factor, but with this approach the S-factor becomes strongly correlated with the assumed branching ratio for  $\beta$ -delayed  $\alpha$ -emission. A recent experiment suggests that the branching ratio may be higher than previously thought, leading to an enhanced S-factor.

The experiment IS605 was performed at the ISOLDE Decay Station (IDS) in May 2016 with the objective of determining the branching ratio for  $\beta$ -delayed  $\alpha$ -emission in the decay of  $^{16}\text{N}$  with a precision of 10% or better. The experiment was very successful: We were blessed with stable running conditions and a high yield of several tens of thousands  $^{16}\text{N}$  ions per second as a molecular beam.

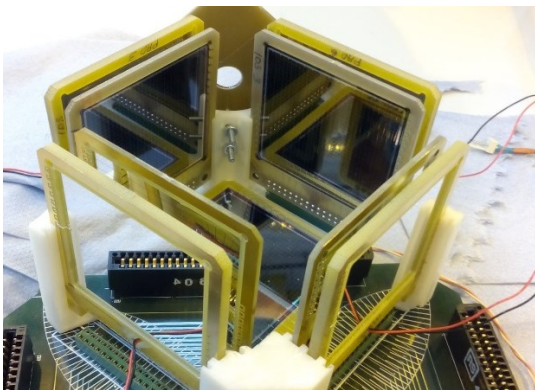


Fig. 1: Setup for detection of charged particles, consisting of five 16x16 DSSDs with thicknesses ranging from 40  $\mu\text{m}$  to 1000  $\mu\text{m}$ . Four of the DSSDs are backed by thick Si Pad detectors.

A compact setup (see Fig. 1) consisting of five 16x16 DSSDs with thicknesses ranging from 40  $\mu\text{m}$  to 1000  $\mu\text{m}$ , was used to detect the  $\alpha$  particles which have energies between 1.0 MeV and 2.2 MeV.

The branching ratio for the  $\alpha$  decay is only of the order of  $10^{-5}$ , making the use of thin detectors imperative, as otherwise the  $\beta$  background would be overwhelming.

Four of the DSSDs were backed by thick Si Pad detectors used to VETO against  $\beta$  particles, thereby further suppressing the background and allowing a clean measurement of the  $\alpha$  spectrum (see Fig. 2). Since the absolute efficiency of each DSSD is precisely known (within a few percent, the efficiency is equal to the solid-angle coverage), the number of  $\alpha$  particles emitted in  $4\pi$  can be reliably deduced from the number of detected  $\alpha$  particles.

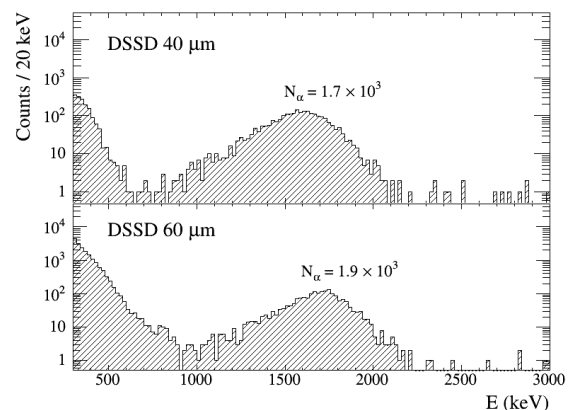


Fig. 2: Energy spectrum measured in two of the DSSDs. The  $\beta$ -delayed  $\alpha$  spectrum extends from 1.0 to 2.3 MeV, while  $\beta$  particles and  $^{12}\text{C}$  recoils account for the intensity below 1.0 MeV. Note that the figure only shows a subset (about 25%) of the acquired data.

The  $\beta$  decay of  $^{16}\text{N}$  gives rise to characteristic  $\gamma$ -ray lines at 2742, 6129 and 7115 keV with well-known intensities, from which the total number of decays can be deduced, given a precise and accurate efficiency calibration of the IDS Ge array. To this end, a rather elaborate calibration scheme was developed, based on a combination of offline and online sources. We expect that this calibration scheme will allow us to determine the efficiency with a precision of at least 5% across the entire energy range.

The data analysis is nearing completion and we expect to publish an improved value for the branching ratio in the near future.

[1] J. Refsgaard et al., [PLB 752, 296-301 \(2016\)](#).

## Study of octupole coupling in $^{207}\text{Tl}$ at the ISOLDE Decay Station

Results of experiment IS588

Website: <http://isolde-ids.web.cern.ch/isolde-ids/>

Tom Berry

(for the IDS collaboration)

One of the defining features of the well-known doubly-magic  $^{208}\text{Pb}$  nucleus is the collective octupole excitation at 2.6 MeV. Such octupole states have also been observed in several neighbouring nuclei [1], and are thought to arise as a result of the presence of many  $\Delta l = \Delta j = 3$  single-nucleon excitations across both the proton and neutron shell gaps. However, the exact composition of the collective excitation is not known. The aim of the IS588 experiments is to investigate states in  $^{207}\text{Tl}$  which arise from the coupling of this octupole vibration with low-lying single proton excitations. This should reveal information on its composition.

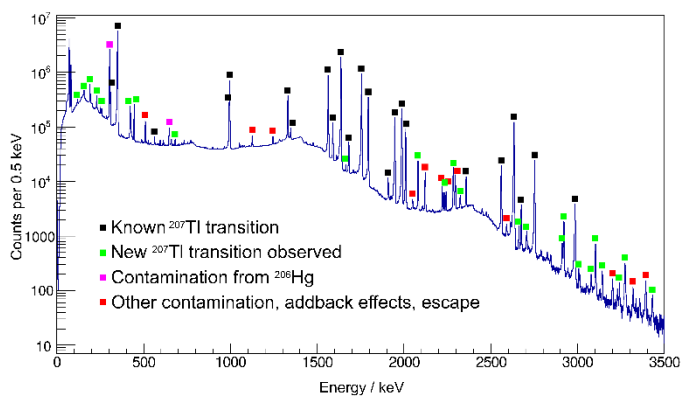


Fig. 1:  $\beta$ -gated  $\gamma$  spectrum for the full  $^{207}\text{Tl}$  data taken in the IS588 experiment in July 2014, up to 3.5 MeV. Significant transitions newly observed in this work are marked in green. Many of the new transitions are not visible here, and were established using  $\beta\gamma\gamma$  coincidence spectra.

Production of  $^{207}\text{Tl}$  through  $\beta$ -decay of  $^{207}\text{Hg}$  has been studied once previously, by Jonson *et al.* at ISOLDE in 1981 [2]. Bombardment of the molten lead target with protons leads to the production of  $^{207}\text{Hg}$ , likely through a secondary reaction. Using this method two IS588 experiments have taken place at IDS. The first, in August 2014, used the four resident HPGe clovers, three plastic beta detectors and a Miniball cluster coaxial with the beam to establish a level scheme using  $\beta\gamma$  and  $\beta\gamma\gamma$  coincidences [3]. The second, in July 2016, used the four clovers plus a fifth off-axis clover from IFIN-HH at a higher  $\gamma$  detection rate. The aim of this second experiment was to provide sufficient statistics for  $\gamma\gamma$  angular correlations, essential for level spin-parity assignments.

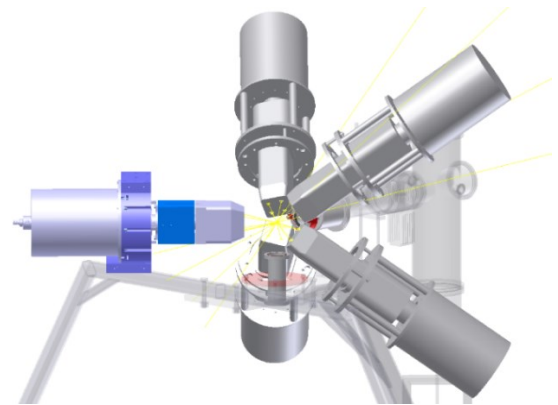


Fig. 2: CAD drawing of IDS in 2016 including the fifth clover from IFIN-HH. Yellow axes pass through crystal face centres and were used to deduce the angles for correlation analysis.

Analysis of the 2014 data has led to a significantly improved level scheme for  $^{207}\text{Tl}$  up to 3632 keV, with four new levels and dozens of new transitions established (spectrum shown in Fig. 1). The advances in detector efficiency relative to the 1981 experiment were crucial. A comprehensive knowledge of the levels in this energy range (between 2.5 and 4.0 MeV) is necessary for the characterization of octupole-coupled states.

A measurement of  $^{208}\text{Hg}$  during the 2016 run has yielded a preliminary  $\beta$ -decay half-life supporting a recent value of 132(50) s achieved at GSI [4], far shorter than the 42 minutes which had been previously suggested.

Current analysis focusses on the angular correlation measurements made in the second experiment. A total of 190 angular pairs exist in the twenty-crystal array, shown in the CAD drawing of IDS in Fig. 2. It is hoped that we will be able to overcome uncertainties on the individual crystal efficiencies to observe reliable angular distributions, leading to spin-parity assignments for the majority of the observed states.

[1] Zs. Podolyák *et al.*, [J. Phys. Conf. Ser. 580, 012010 \(2015\)](#).

[2] B. Jonson *et al.*, CERN-81-09, 640 (1981).

[3] R. J. Carroll, ISOLDE Newsletter 2015, page 24.

[4] R. Caballero-Folch *et al.*, [PRL 117, 012501 \(2016\)](#).

## Beta-delayed fission in $^{188}\text{Bi}$ and shape-coexistence and shape-evolution studies for bismuth isotopes by in-source laser spectroscopy

Results of experiment IS608

A. N. Andreyev, A. E. Barzakh

(for the Windmill-RILIS-ISOLTRAP-COLLAPS collaboration)

In June-July 2016 a successful investigation of bismuth isotopes (IS608) was performed by our collaboration. The experiment focused on two main goals: 1) the study of shape-coexistence and shape-evolution phenomena in the long chain of bismuth isotopes ( $^{187-218}\text{Bi}$ ) via isotope shift (IS) and hyperfine structure (hfs) measurements by in-source laser spectroscopy, and 2) beta-delayed fission ( $\beta\text{DF}$ ) studies of two isomerically-separated states in  $^{188}\text{Bi}$ . The experiment greatly benefitted from the use of two complementary techniques for photo-ion current monitoring: the Windmill (WM) system for short-lived alpha-decaying nuclei and Multi-Reflection Time of Flight Mass Separator (MR-ToF MS) for longer lived isotopes. During an additional run in September 2016, as a part of the IS608 program, hfs measurements for several isotopes in the range of  $^{196-209}\text{Bi}$  were performed by COLLAPS. The purpose was to clarify the possible existence of isomeric states and to measure the hyperfine anomaly (hfa) in these Bi isotopes. Besides the valuable information on the magnetization distribution in nuclei, the knowledge of the hfa is crucial for the proper analysis of the data obtained for the other Bi isotopes.

Following the preliminary analysis of the IS608 data, the Bi electromagnetic moments and the changes of the charge radii,  $\delta\langle r^2 \rangle$ , were obtained for bismuth isotopes with  $A = 187-191, 194-202, 214-218$  (in total 27 isotopes). The most interesting findings are as follows:

1. In contrast to the previous conclusions on sphericity of the  $9/2^-$  g.s for the light Bi isotopes, based on decay and in-beam studies, a gradual onset of deformation in the  $9/2^-$  g. s. of the lightest isotopes was deduced, up to  $\langle \beta^2 \rangle^{1/2} \sim 0.18$  in  $^{187}\text{Bi}$ . The radii for the  $9/2^-$  Bi ground states start to deviate from the nearly-spherical trend of the lead isotopes at  $N = 108$  ( $^{191}\text{Bi}$ ) when moving to lower neutron numbers. Our conclusions are substantiated by the quadrupole moment values measured in the same IS608 experiment.

2. A large isomer shift, corresponding to a more deformed configuration for intruder Bi isomers ( $I^\pi=1/2^+$ ) for  $^{191,199,201}\text{Bi}$  was observed.

3. A pronounced shape staggering/coexistence at  $A = 188$  (Fig. 1) was found. This phenomenon is similar to the famous Hg shape staggering/coexistence [1]. It appears at the same  $N$  and has nearly the same magnitude.

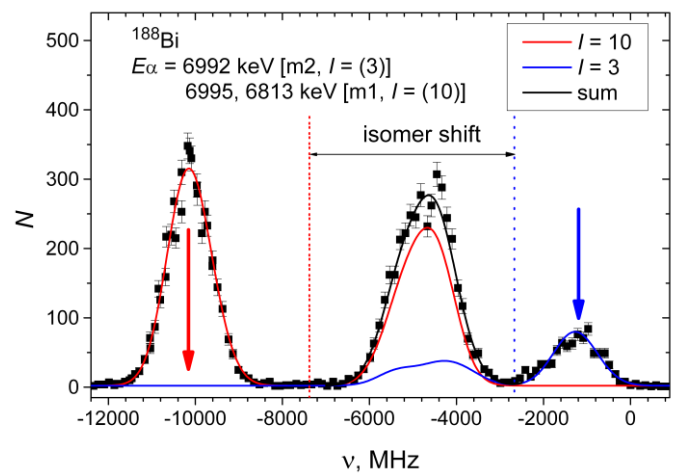


Fig. 1: Hyperfine structure spectra for  $^{188m1,188m2}\text{Bi}$ . The large isomer shift points to a deformation jump for low-spin  $^{188}\text{Bi}$  isomer.

4. A marked deviation from the presumed linear systematic trend for  $\mu(9/2^-)$  in  $^{215,217}\text{Bi}$  was found. Along with the indication of the inverse odd-even staggering in radii near  $^{216}\text{Bi}_{133}$  this may be connected with the influence of the octupole degree of freedom near  $N = 133$ .

5. Fission fragment mass distributions and  $\beta\text{DF}$  probabilities for isomerically separated states in  $^{188m1,188m2}\text{Bi}$  were deduced. Isomer selectivity was achieved by the tuning of the narrow-band laser frequency to the first hfs peak for high-spin isomer studies and to the third hfs peak for low-spin isomer (see arrows in Fig. 1). This enabled us, for the first time, to investigate the spin-dependence of the  $\beta\text{DF}$  process and to check theoretical predictions of asymmetrical fission fragment mass-distributions in this region of nuclei.

[1] G. Ulm et al., *Z. Phys. A* **325**, 247 (1986).

## Search for scalar currents in the $\beta$ -delayed proton decay of $^{32}\text{Ar}$

Letter of Intent INTC-I-172

B. Blank, N. Severijns  
(for the WISARD collaboration)

Most  $\beta\nu$  angular correlation experiments searching for scalar weak currents measure the recoil-energy distribution of the daughter nucleus. For the new WISARD (Weak-interaction studies with  $^{32}\text{Ar}$  decay) experiment [1], the Doppler effect on  $\beta$ -delayed protons will be measured. Scalar currents and the Standard Model vector currents have different angular distributions between the two emitted leptons: angular correlations peak at 0 degrees for the vector current and at 180 degrees for the scalar current. The recoil of the daughter nucleus is thus almost zero on average for a scalar decay, whereas it is maximum for a vector decay. In  $\beta$ -delayed proton decay, the protons are emitted from a moving source imposing a Doppler effect on their energy. The proton energy peak is thus broadened in the case of a vector current, whereas it remains much narrower for a purely scalar current. This property has been used in an earlier experiment at ISOLDE yielding a value of  $a = 0.998(5)$  for the  $\beta\nu$  angular correlation coefficient [2] in agreement with the Standard Model expectation of unity.

The WISARD experiment [1] will measure the emitted positron and proton in coincidence (see Fig. 1). Positrons and protons will be detected either in the same or in opposite hemispheres with respect to the catcher foil. Thus for a vector current, for which the positron and the neutrino are emitted preferentially in the same direction, the daughter nucleus which emits the proton has a recoil preferentially in the opposite direction. Therefore, a proton emitted in the same direction as the positron will have a reduced energy, whereas a proton emitted in the opposite direction compared to the positron will see its energy boosted by the recoil. For a scalar current, for which the positron and the neutrino are emitted preferentially in opposite directions, the average recoil of the daughter nucleus is zero. Therefore, detecting the proton and the positron in the same or in the opposite hemisphere does not change the proton energy. Thus, instead of measuring a Doppler broadening, the WISARD experiment will measure a Doppler shift in one or the other direction, which provides increased sensitivity.

Initial Monte-Carlo simulations performed to study the sensitivity of the proposed experiment clearly show the

effect expected provided the experimental energy resolution is sufficiently good, i.e. about 10 keV or better. Simulations with a mixture of scalar and vector contributions can give indications with respect to the final precision of the correlation coefficient  $a$ . At this stage, relatively simple simulations have shown that a scalar contribution in the decay to the isobaric analogue state (IAS) in the input of the simulations as low as 0.1% can be found when fitting the resulting shape of the IAS with freely varying contributions of scalar and vector currents. These simulations will be refined to include more realistic conditions in a full GEANT4 simulation.

The WISARD experiment will use the former WITCH setup which is currently being modified and upgraded.

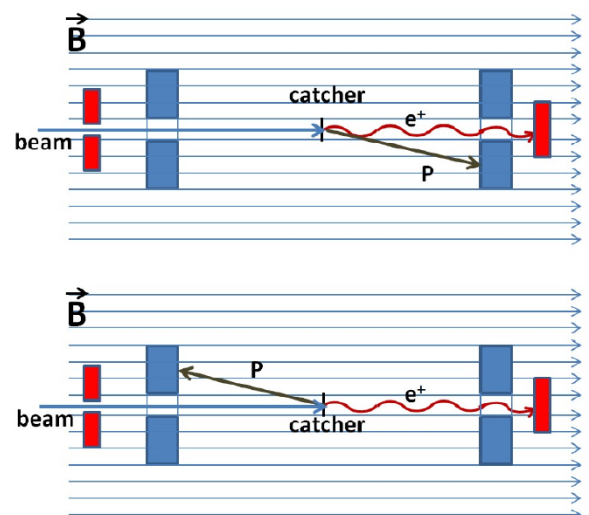


Fig. 1: Schematic view of the proton detectors (in blue) and positron detectors (in red) to be installed on both sides of the catcher foil in the center of the WITCH magnet, for the new WISARD experiment. The positrons will spiral along the magnetic field lines with their bending radius preventing them from ending up on the proton detectors.

[1] B. Blank et al., Letter of Intent, CERN-INTC-2016- 050 (INTC-I-172).

[2] E. G. Adelberger et al., [PRL 83, 1299 \(1999\)](#).

# RIB applications to medical and solid-state physics

## $^{68m}\text{Cu}/^{68}\text{Cu}$ as a new probe for hyperfine studies

Experiment IS585

<https://espace.cern.ch/ISOLDE-SSP>

*A.S. Fenta, J.G. Correia, M.R. da Silva, Lars Hemmingsen  
and L.M.C. Pereira (for the SSP collaborations)*

Known to some of the oldest civilizations on record, Copper (Cu) accompanies human living, technology and arts since countless times with increased relevance in our highly technological world. From coins, electrical equipment and construction to agricultural pesticides, e.g., as an algicide in water purification, Cu is omnipresent in our ecosystem. A biological factor and a particular key element for humans, Cu additionally plays an important role as a cofactor for numerous enzymes and proteins, crucial for respiration, iron transport and metabolism, cell growth, and homeostasis. Evidently, there is a large interest in techniques, which could be used to follow and characterize Cu atoms behaviour and its chemical bonds at the atomic scale.

Copper has 2 stable isotopes,  $^{63}\text{Cu}$  and  $^{65}\text{Cu}$  [1-2]. Both have been used very successfully in NMR/NQR studies of bulk matter, notably recently in HT superconductors. Such experiments, however, require a large amount of sample material and are often restricted to low temperatures. For investigating impurity problems or rare biological materials, a highly sensitive nuclear technique like Mossbauer (MS) or Time-Differential Perturbed Angular Correlation (TDPAC) spectroscopy would be necessary. Unfortunately, no copper isotope is available for MS experiments. Also for TDPAC, to date, no suitable case has been studied. The development of modern radioactive on-line isotope separator techniques has, however, widened the spectrum of radioactive nuclei available for such experiments. At the ISOLDE facility, the copper isotopes from  $^{59}\text{Cu}$  to  $^{74}\text{Cu}$  are available as a result of the progressive development of on-line ion-source techniques. They have already been successfully used in studies of their ground (and long-lived isomeric) state nuclear moments. If one looks at candidates for TDPAC in the decay schemes of these copper isotopes, one finds that  $^{68m}\text{Cu}$  could be suitable. Its decay cascade

appears as the best candidate to be used as a copper hyperfine probe for applications in several fields of physics, chemistry and biophysics.

In December 2014, TDPAC experiments were performed for the first time using the decay of  $^{68m}\text{Cu}$  ( $6^-$ , 721 keV, 3.75 min), produced and measured on-line at ISOLDE. The intermediate state ( $2^+$ , 84.1 keV, 7.84 ns) offers the unique opportunity to study electromagnetic fields interacting with a copper probe in materials via hyperfine interactions. The analysis and resulting publication were completed in 2016 [3], and that article was selected as a EPL's highlight of 2016. The determination of the nuclear moments of this state was based on  $^{68m}\text{Cu}$  implantation into suitable target materials:  $\text{Cu}_2\text{O}$  pellets for the electric quadrupole moment  $|Q(2^+, 84.1 \text{ keV})| = 0.110(3) \text{ b}$ ; cobalt and nickel foils for the magnetic dipole moment  $|\mu| = 2.857(6) \mu_N$ . The results were discussed in the framework of shell model calculations and the additivity rule for nuclear moments with respect to the robustness of the  $N = 40$  sub-shell. Future experiments using  $^{68m}\text{Cu}$  will benefit from the ability to tune the laser ion source to optimize the production of the  $^{68m}\text{Cu}$  ( $6^-$ ) isomeric state, regarding the  $^{68m}\text{Cu}$  ( $1^+$ ) ground state [4]. By demonstrating the feasibility of  $^{68m}\text{Cu}/^{68}\text{Cu}$  experiments, and determining the nuclear moments with high precision, this work established a completely new isotope for TDPAC studies in a wide range of fields, from solid state physics to chemistry and biophysics.

The success of these experiments motivated the development of a new on-line TDPAC setup dedicated to experiments with short-lived isotopes. The design has been completed in the meantime (Fig. 1); production and commissioning are foreseen for 2017. This setup will allow for easy sample exchange, in-situ thermal annealing, and measurements at high-temperature. Among other potential applications, we highlight a novel

class of spintronic materials: antiferromagnetic semiconductors of the type CuMnAs.  $^{68\text{m}}\text{Cu}$  PAC can be used to determine the Néel temperature ( $T_N$ ), for example, as a function of composition in  $\text{CuMnAs}_{1-x}\text{Sb}_x$  and  $\text{CuMnAs}_{1-x}\text{P}_x$ . Conventional magnetometry techniques are not suitable since the antiferromagnetic-paramagnetic transition is not easily discernible in materials with such high  $T_N$  (of the order of 480 K in CuMnAs). Neutron diffraction, a typical alternative when investigating bulk materials, is also inconvenient in this case due to the long measurement times required for thin films. The PAC-SLI setup would be particularly useful in this case allowing implantation and/or annealing at high temperature and measurements to be performed at elevated temperatures. On the other hand, works concerning chemical/biochemical samples require liquid support allowing the  $^{68\text{m}}\text{Cu}$  to diffuse to the desired binding site on molecules. The PAC-SLI setup has been designed to allow the full exchange of the sample holder and handling systems, e.g. between solid state and liquid-like samples. To reduce sublimation with sample losses and inherent congelation, liquid samples require higher pressures than  $10^{-3}$  mbar and, consequently, the further installation of a multistage differential pumping station, isolating the ISOLDE beam line under  $10^{-6}$  mbar vacuum. The optimized system is still being discussed, which is the reason why we envisage tests using ionic liquid solutions, which have very low vapour pressure. Such samples can be placed in the present system and

vacuum beam line, providing the necessary experience on PAC experiments looking at Cu(I) binding to anions and molecules dissolved in liquids.

Note: this work is part of the doctoral thesis of Abel S. Fenta, to be defended in 2017 (U. Aveiro and KU Leuven).

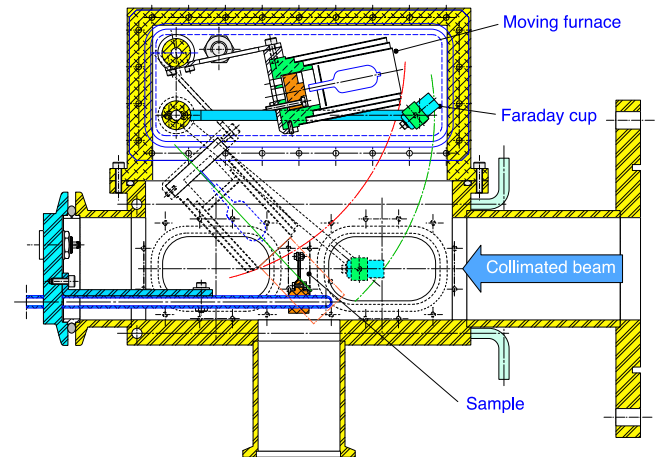


Fig. 1: Schematic drawing of the new setup dedicated to TDPAC online experiments with short lived isotopes at ISOLDE. To be produced and commissioned in 2017.

- [1] Interactive Chart of Nuclides, National Nuclear Data Center, retrieved 8 April (2011).
- [2] P. Vingerhoets et al., [PRC 82, 064311 \(2010\)](#).
- [3] A. S. Fenta et al., [EPL 115, 62002 \(2016\)](#).
- [4] L. Weissman et al., [PRC 65, 024315 \(2002\)](#).

## Lattice location of $^{27}\text{Mg}$ in differently doped GaN

Results of experiment IS453

Ulrich Wahl

(for the EC-SLI collaboration)

Mg-doped  $p$ -type GaN is nowadays a core component of many optoelectronic devices which we find in our homes, e.g. LEDs for solid state white lighting or blue lasers. Yet there are some basic properties related to  $p$ -type doping of GaN that are still poorly understood and also limit the performance of devices. One such major problem is an inherent doping limit: once the Mg concentration in GaN surpasses  $\sim 10^{19}\text{-}10^{20}\text{ cm}^{-3}$ , further introduction of Mg does not lead to an increase in the hole concentration. Recently a theory has been put forward [1] that explains this behaviour by suggesting an amphoteric nature of Mg: once the doping limit has been reached, additional Mg atoms are not incorporated on substitutional Ga sites any more (where they act as acceptors) but on interstitial

sites (where they form compensating Mg; double donors).

The emission channeling technique with short-lived isotopes (EC-SLI) gives direct information on the lattice location of radioactive impurities implanted into single crystals. EC-SLI with  $^{27}\text{Mg}$  ( $t_{1/2}=9.5$  min) produced at ISOLDE hence offers the unique opportunity of studying the Mg lattice location in GaN and other nitride semiconductors such as AlN and InN.

We present recent results from our 2016 beam time on  $^{27}\text{Mg}$  in different doping types of GaN (undoped, Si-doped  $n$ -type, Mg-doped  $p$ -type, Mg-doped as grown). After implantations between room temperature and  $300^\circ\text{C}$ , the majority of  $^{27}\text{Mg}$  occupies the substitutional Ga sites, however, significant fractions were found on

interstitial positions  $\sim 0.6 \text{ \AA}$  from ideal octahedral sites (Fig. 1, [2]). The interstitial fraction of Mg was correlated with the GaN doping character, being highest (up to 30%) in samples that were doped *p*-type with  $2 \times 10^{19} \text{ cm}^{-3}$  stable Mg during epilayer growth, and lowest in Si-doped *n*-GaN, thus giving direct evidence for the amphoteric character of Mg. Implanting above  $400^\circ\text{C}$  converts  $^{27}\text{Mg}_i$  to  $^{27}\text{Mg}_{\text{Ga}}$  and the temperature dependence of the interstitial fraction  $f_i(T)$  in the GaN:Mg sample was used to estimate the migration energy ( $E_M$ ) of  $\text{Mg}_i$  applying two simple Arrhenius models. Assuming that  $\text{Mg}_i$ , vibrating with an attempt frequency  $\nu_0 \sim 2 \times 10^{13} \text{ Hz}$ , starts to migrate due to its thermal energy and that it requires a certain number of jumps  $N$  until it encounters a Ga vacancy during the life time  $\tau = 13.6 \text{ min}$  of  $^{27}\text{Mg}$ , which will lead to the formation of  $\text{Mg}_{\text{Ga}}$ , following the Arrhenius relation

$$f_i(T) = f_{i0} \exp \left[ -\frac{\nu_0 \tau}{N} \exp \left( -\frac{E_M}{k_B T} \right) \right].$$

$N$  was assumed either 1 or  $10^5$ , where  $N=1$  represents the limiting case in which  $\text{Mg}_i$  has a neighbouring Ga vacancy, and  $N=10^5$  is the upper limit when the diffusion-induced widening of the  $\text{Mg}_i$  profile becomes comparable to the implantation depth. According to the least square fits for  $E_M$  shown by the solid lines in Fig. 1, the migration energies are thus estimated between 2.0 eV ( $N=1$ ) and 1.3 eV ( $N=10^5$ ), respectively.

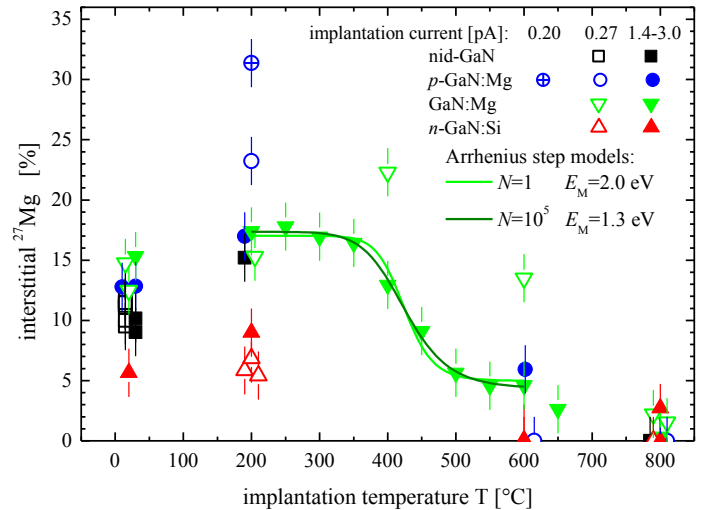


Fig. 1: Interstitial fractions of  $^{27}\text{Mg}$  in the four different types of GaN samples as a function of the implantation temperature. Open symbols were implantations at low beam currents of 0.20-0.27 pA, while filled symbols were measured at 1.4-3.0 pA. The solid lines show the fractions using two Arrhenius models:  $N$  is the assumed number of jumps and  $E_M$  the activation energy for migration. From [2].

- [1] G. Miceli and A. Pasquarello, [PRB 93, 165207 \(2016\)](#).  
 [2] U. Wahl, L. M. Amorim, V. Augustyns, A. Costa, E. David-Bosne, T. A. L. Lima, G. Lippertz, J. G. Correia, M. R. da Silva, M. J. Kappers, K. Temst, A. Vantomme, and L. M. C. Pereira, [PRL 118, 095501 \(2017\)](#).

## Cd and In-doping in $\text{SnO}_2$ gas sensor by means of the TDPAC technique

Results of experiment LOI144

Submitted to the Journal of Applied Physics, January 2017

*J. Schell and A. W. Carbonari  
(for the SSP collaboration)*

Among several semiconducting oxides,  $\text{SnO}_2$  is intensively applied as a sensor material with sensing performance being enhanced by metal doping. The present work focuses on the Time Differential Perturbed gamma-gamma Angular Correlations (TDPAC) method to study dopant incorporation during synthesis and by implantation of In and Cd metals. The hyperfine field parameters have been probed as a function of temperature and thermal treatments in thin film and powder/pellet samples. The TDPAC results reveal that  $^{117}\text{Cd}/\text{In}$  is incorporated into, and stabilized, in the  $\text{SnO}_2$  lattice for the cation substitutional site, an advantage for many applications, particularly as a gas sensor.

Figure 1 shows the PAC observable function  $R(t)$  obtained after implantation of  $^{117}\text{Ag}$  into the  $\text{SnO}_2$  thin film

and decay to  $^{117}\text{Cd}$  with subsequent 5 minutes air annealing at 973 K. The result shows evidence for the  $^{117}\text{In}$  probe nuclei interacting with two different local environments as revealed by the two observable frequencies  $\omega_1 = 390.0(5) \text{ Mrad/s}$  and  $\omega_2 = 50.8(4) \text{ Mrad/s}$ , respectively. From the experimental pattern there is no evidence for observable magnetic interaction, therefore the frequencies are due to different fractions of probe nuclei,  $f_1 = 57.4 (1) \%$  and  $f_2 = 43.2 (1) \%$  interacting with different Electric Field gradients (EFG)<sub>1</sub> and EFG<sub>2</sub>. Since the probe excited state has spin 3/2, in the absence of magnetic field, there is only one observable frequency and  $\omega_0$  and  $\eta$  cannot be separately identified. Therefore, density functional theory was used with the full potential L/APW+lo method implemented in the WIEN2k code [1], to simulate the electric field

gradient parameters at the In probe occupying a Sn substitutional site. The lattice constants were fixed to the experimental values of the pure compound [2], and all the free fractional atomic coordinates were optimized. A 2x2x3 supercell ( $a=b=13.40$  Å,  $c=9.56$  Å) of the SnO<sub>2</sub> host was considered, where one of the Sn atoms was replaced by the In impurity. The GGA-PBE approximation for the exchange-correlation functional was used [3]. The data was then fitted with fixed  $\eta_1 = 0.24$  (neutral) or  $\eta_1 = 0.34$  (+1 e<sup>-</sup>) for the EFG<sub>1</sub> field. Under these assumptions  $\omega_{01} = 386.0(4)$  Mrad/s ( $\eta_1 = 0.24$ ) or  $\omega_{01} = 382.7(2)$  Mrad/s ( $\eta_1 = 0.34$ ), were obtained, corresponding to  $|V_{zz1}| = 8.6(1) \cdot 10^{21}$  V/m<sup>2</sup> or  $|V_{zz1}| = 8.5(1) \cdot 10^{21}$  V/m<sup>2</sup>. Clearly, the different axial asymmetry parameters  $\eta_1$  now used and fixed during the fit have little influence on the obtained  $V_{zz}$  values. The ~25% differences between the “experimental”  $V_{zz}$  and the simulated ones ( $6.87 \times 10^{21}$  V/m<sup>2</sup> or  $6.59 \times 10^{21}$  V/m<sup>2</sup>) are quite reasonable to accept since an increase of simulated  $V_{zz}$  is expected to occur upon the increase of the supercell size requiring a much longer calculation. Based on this analysis EFG<sub>1</sub> is tentatively assigned to <sup>117</sup>In atoms occupying substitutional sites of the SnO<sub>2</sub> lattice.

The results were crucial to the data clarification and conclusion of the doctoral thesis of Juliana Schell. Therefore, we intend to submit a full proposal within the current year 2017, organized as an international

collaboration bringing together key people and new materials with potential application as gas sensors.

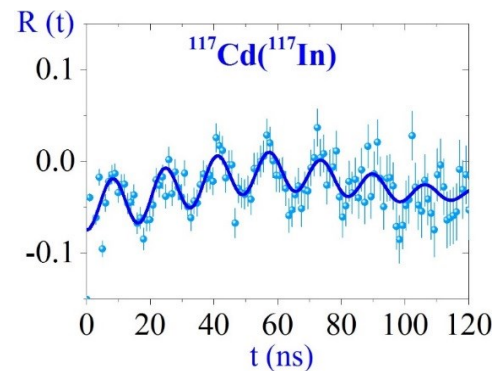


Fig. 1: PAC spectrum of a SnO<sub>2</sub> thin film of 100 nm thickness using <sup>117</sup>Cd/<sup>117</sup>In and after heat treatment for 5 minutes in air at 973 K.

- [1] P. Blaha, K. Schwarz, G. K. H. Madsen, D. Kvasnicka, and J. Luitz, WIEN2K: An Augmented Plane Wave+Local Orbitals Program for Calculating Crystal Properties (Karlheinz Schwarz, Technische Universität, Wien, Austria, 1999).
- [2] A. A. Bolzan, C. Fong, B. J. Kennedy and C. J. Howard, *Acta Crystallographica B* **53**, 373 (1997).
- [3] P. Perdew, K. Burke, and M. Ernzerhof, *PRL* **77**, 3865 (1996).

## A new laser polarization setup at ISOLDE

Results of experiment LO1168

Wouter Gins

(for the laser-polarization team at ISOLDE)

Spin-polarized beams of radioactive isotopes are interesting for many fields of research, as stated in [1]. Here we report on the commissioning of a new ISOLDE setup for the production of such beams using resonant laser optical pumping. We plan to use this set-up for a variety of applications, such as  $\beta$ - $\gamma$  correlation studies for fundamental interaction research or  $\beta$ -detected NMR for biophysics research.

This beamline shares design aspects with the COLLAPS setup for laser-polarization, and we use the results from that setup as a benchmark. Based on the new design (Fig. 1), the beam line elements were constructed and installed in summer 2016. During the last day of protons for ISOLDE in 2016,  $\beta$ -asymmetry spectra on polarized <sup>26,28</sup>Na were recorded. Asymmetries of 28% and 59% (Fig. 2) were observed for <sup>26,28</sup>Na respectively,

comparable to 39% and 59% observed previously at COLLAPS [2]. Thus, we are confident in stating that we can start our physics program.

The beamline in its current configuration will be used for the first phase of IS601, which studies the  $\beta$ -asymmetry parameter of <sup>35</sup>Ar. The study of this asymmetry is crucial to reduce the uncertainty in the  $V_{ud}$  element of the CKM matrix. A smaller uncertainty is important for the unitarity test of this matrix, which results in tighter constraints on contributions from beyond Standard Model physics.  $\beta$ - $\gamma$  correlations will not yet be measured in this first phase, which focuses on identifying the most appropriate implantation crystal and temperature for maintaining the <sup>35</sup>Ar polarization for a sufficiently long time. Further phases of the experiment do require these correlation measurements, which will make the measured



asymmetry sensitive to only the  $\beta$ -decay to the ground state of  $^{35}\text{Cl}$ . Upgrading the beamline with a dedicated and efficient  $\beta$ - $\gamma$ -detection set-up is thus necessary before moving to the next phase.

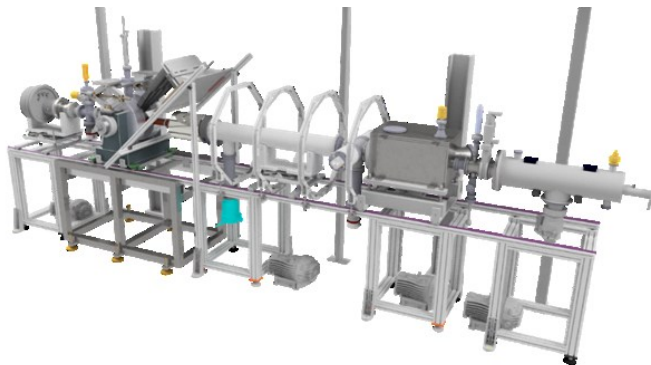


Fig. 1: CAD picture of beamline mounted at ISOLDE as of November 2016.

Turning from fundamental symmetries to biology, laser-polarized nuclei will also be used for  $\beta$ -NMR studies of metal-ion interaction with biomolecules (IS582 and IS583). Extracting a chemical shift from these measurements will provide information about the binding site and dynamics in biomolecules. As a first step towards  $\beta$ -NMR in liquid samples, tests will be performed

on different ionic liquids to investigate the limits of this approach. Upgrades to the beamline will include an efficient vacuum-liquid interface and an NMR chamber that can host liquid samples.

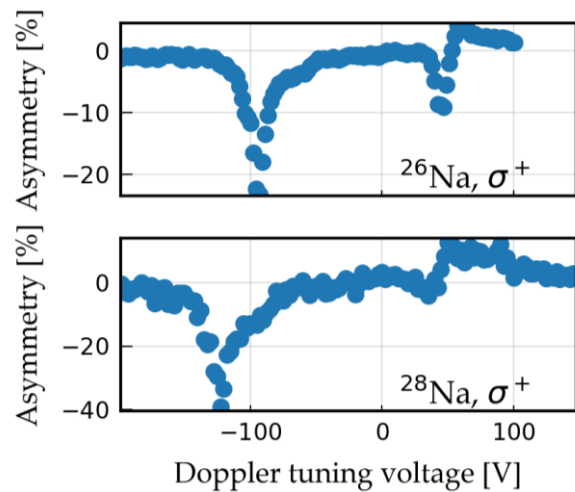


Fig. 2: Obtained  $\beta$ -asymmetry spectra during the November run.

[1] R. Garcia Ruiz et al, [EPJ Web of Conf. 93, 07004 \(2015\)](https://doi.org/10.1051/epjconf/20159307004).

[2] M. Kowalska et al, New laser polarization line at the ISOLDE facility, submitted to Journal of Physics G (2017)

## 20 years of $^{57}\text{Mn}$ (1.5 min.) for $^{57}\text{Fe}$ emission Mössbauer spectroscopy

Results of experiments IS359, IS426, IS443, IS501, IS576, IS578

Website: <http://e-ms.web.cern.ch/>

*H. P. Gunnlaugsson  
(for the Mössbauer collaboration at  
ISOLDE/CERN)*

Mössbauer spectroscopy is a unique interrogation technique in solid state physics, giving access to quantities that are either difficult or impossible to obtain with conventional methods. The technique uses resonance detection of gamma emission from low lying nuclear state which allows detection with energy resolution dictated only by the uncertainty relationship ( $\sim 5$  neV in the case of  $^{57}\text{Fe}$ ). This resolution is sufficient to resolve the so-called hyperfine interactions, the interactions between the nucleus and the electron configuration of the atom, that in praxis are used to determine the electronic configuration of an atom.

$^{57}\text{Fe}$  has the most applied Mössbauer transition ( $>90\%$  of the literature). Experiments utilising this transition require, however, local concentration  $\sim 0.1\%$  of  $^{57}\text{Fe}$  which makes impurity studies difficult. This is overcome in emission Mössbauer spectroscopy (eMS), where concentrations down to  $10^{-4}$  at.% can be measured. There are three

mother elements which make eMS feasible with  $^{57}\text{Fe}$  as the end product,  $^{57}\text{Mn}$ ,  $^{57*}\text{Fe}$  and  $^{57}\text{Co}$ .

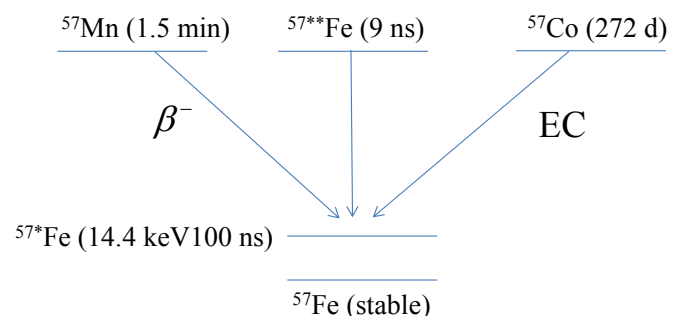


Fig. 1: Decays to the 14.4 keV Mössbauer state of  $^{57}\text{Fe}$ .

Experiments using  $^{57}\text{Co}$  are difficult due to the long lifetime, which results in a possible precipitation. Also, the fact that  $^{57}\text{Co}$  decays with electron capture leaves the electronic configuration of the Fe atom in a highly excited state. Despite this, many experiments are performed

each year with the commercially available  $^{57}\text{Co}$ .

Experiments using  $^{57}\text{Fe}$  have been performed using Coulomb excitation and recoil implantation, most recently at the Hahn-Meitner institute in Berlin [1]. These experiments, however, yielded ambiguous or incomplete results since the spectra were measured only for  $\sim 100$  ns after the implantation process. In some cases this is not enough time to anneal the implantation damage. Still, good results were obtained, for example, for interstitial Fe impurities in metals [2].

Many problems with  $^{57}\text{Co}$  and  $^{57}\text{Fe}$  are overcome by using  $^{57}\text{Mn}$  as the mother element. Initial tests were performed at ISOLDE 2, in 1989. However, the beam had a dominating fraction of the stable  $^{57}\text{Fe}$  ( $>99\%$ ) [3], demonstrating the need for ionization that was *element specific*. This was achieved with RILIS at ISOLDE-3 [4].

Emission Mössbauer spectroscopy using  $^{57}\text{Mn}$  has several benefits as compared to conventional Mössbauer spectroscopy and eMS using  $^{57}\text{Fe}$  and/or  $^{57}\text{Co}$ . First, one can measure concentrations down to  $10^{-4}$  at.%. This low concentration ensures that the probe atoms do not precipitate and can be regarded as probes of the host material. Second, in the  $\beta^-$  decay of  $^{57}\text{Mn}$ , the daughter  $^{57}\text{Fe}$  is given an average recoil of 40 eV which in some cases is sufficient to expel the probe atom from its lattice site into interstitial sites. Thus a study of interstitial defects is feasible, which would under normal circumstances not be possible due to thermodynamic constraints.

In the first test experiments performed in 1996, spectra were measured in a transmission mode. It was quickly realized that the beam was more intense than expected, with an intensity of about  $3 \times 10^8$  ions/s, which resulted in unstable performance of conventional proportional counters. This led to the use of parallel plate resonance detectors equipped with stainless steel electrodes enriched in  $^{57}\text{Fe}$ , which were first used already in 1997, and have been employed ever since.

Equipment used for the measurements has been gradually upgraded in the last 20 years. The high intensity of the beam requires rapid sample changes (every  $\sim 1/2$ -2 hours). This has been met by utilizing different sample installations that can be exchanged within 10-15 minutes. The most recent upgrade, has been an equipment to allow for rapid exchange of

samples (removal of sample in  $\sim 5$ -10 seconds, start of implantation into next sample in  $\sim 30$  seconds) which allows measurements of samples outside the implantation chamber, securing a wider range of sample environments, such as rapid cooling and measurements at low temperatures to be employed.

The first Mössbauer experiments concentrated on group IV semiconductors, in particular silicon (experiments IS359 and IS426). Amongst the main results obtained was the determination of charge-state dependence of the diffusivity of interstitial Fe in silicon [5] which had been disputed in the literature.

Around 2005 the prospects of dilute magnetic semiconductors drew much attention following theoretical predictions of Dietl et al., [6] (IS443 & IS501). Here, eMS played an important role since precipitation of probe atoms is avoided and thus local information on magnetic properties can be obtained. Many interesting phenomena in oxide- and nitride- semiconductors were observed, however no signature of dilute magnetism was found [7].

The interesting physics of oxide semiconductors resulted in a specific experiment on the (AlGa)N:Mn system (IS576). New Mn-based magnetic materials resulted in experiments dealing with manganese-based alloys (IS578). In both cases, measurements and publications are still on-going, although the results obtained on the (AlGa)N system have led to a new line of experiment concentrating on (InGa)N semiconductors (IS630).

Currently, there are ideas of performing wet chemistry experiments using  $^{57}\text{Mn}$  as a precursor. As manganese can be stabilized in different charge states compared to iron, one can effectively generate different iron oxide species by using the  $^{57}\text{Mn} - ^{57}\text{Fe}$  radioactive decay that cannot be produced with common chemical methods.

- [1] R. Sielemann and Y. Yoshida, [Hyperfine Interact. 68, 119 \(1992\)](#).
- [2] R. Sielemann, [Hyperfine Interact. 80, 1239 \(1993\)](#).
- [3] G. Langouche et al., [CERN-ISC-92-41; ISC-I-4 \(1992\)](#).
- [4] V. N. Fedoseyev et al., [NIM 126, 88 \(1997\)](#).
- [5] H. P. Gunnlaugsson et al., [Appl. Phys. Lett. 80, 2657 \(2002\)](#).
- [6] T. Dietl et al., [Science 287, 1019 \(2000\)](#).
- [7] R. Mantovan et al., [Adv. Electr. Mater. 1, 1400039 \(2015\)](#).

## Studies with post-accelerated beams

### Reaction study of neutron rich Li isotopes

IS561 takes the first beam to the HIE-ISOLDE XT02 beamline

*Jesper H. Jensen  
(for the IS561 collaboration)*

**IS561:** In spite of the intense work done over the last 30 years, the structure of the excited states of halo nuclei is highly debated. The increase of beam energy of HIE-ISOLDE now allows us to explore these states and the neighbouring resonances via transfer reactions to higher excitations than for which REX-ISOLDE allowed.

The goal of IS561 is to study the (t,p) two-neutron transfer to  ${}^9\text{Li}$  populating the ground state of  ${}^{11}\text{Li}$  as well as low-lying resonances. We aim at detecting the charged particles from the transfer reactions as well as neutrons coming from the decay of possible  ${}^{11}\text{Li}$  resonances, for this reaction we need a  ${}^9\text{Li}$  energy of at least 7.5 MeV/u.

In 2016 the new equipment was installed on the XT02-beamline but HIE-ISOLDE was in its start-up phase and there was not yet sufficient energy for the (t,p) reaction. Hence, we spent the first part of our beam time on the  ${}^9\text{Li}$  (d,p) reaction with two goals in mind. Firstly to assess the beam properties and optimize the setup and secondly to provide experimental result for  ${}^{10}\text{Li}$ , an important piece in the puzzle of understanding  ${}^{11}\text{Li}$ .

**The setup:** The experiment was performed in the newly installed Scattering Experiment Chamber (SEC) on the XT02 beam line of HIE-ISOLDE.

The charged particle setup, as shown in Fig. 1, consisting of a pentagon structure holding highly segmented  $\Delta E$ -E-telescopes forming a barrel ended by an annular-radially segmented Silicon detector (Micron: S3). The telescopes are formed by Double Sided Si Strip detectors DSSD (Micron: W1), each with 256 pixels of  $3 \times 3 \text{ mm}^2$ . The detectors cover a large solid angle in the forward direction (S3:  $8^\circ - 30^\circ$ , W1:  $45^\circ - 80^\circ$ ). Coincidences between heavy fragments in the S3 and light fragments in the pentagon give information on the beam properties, important in order to optimize the resolution of the set-up. In the backward direction, covering  $120^\circ - 150^\circ$ , a bigger DSSD (Micron: BB7) with 1024 pixels of  $2 \times 2 \text{ mm}^2$  was

placed. For neutron detection, the SAND-array was placed 2 m downstream of SEC. SAND consists of 30 plastic scintillators operated in ToF mode, using charged particles detected in the BB7 as a start signal.

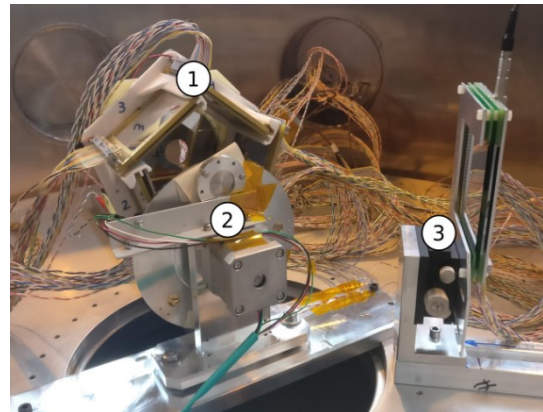


Fig. 1: *Experimental setup.* 1)  $\Delta E$ -E telescopes in a pentagon barrel structure ended by annular-radially sectored S3-detector. 2) Motor controlled target wheel. 3) BB7 telescope in the backward direction.

**The Experiment:** The  ${}^9\text{Li}^{3+}$  beam was accelerated to the record HIE-ISOLDE beam energy of 6.72 MeV/u. The estimated rate during the run was  $10^4$   ${}^9\text{Li}$ /s. Without stripping foils at the bend to XT02 a  ${}^{12}\text{C}$ -contamination of the order of  $10^7$ /s was present. Inserting the stripping foils, this contamination was reduced by at least 4 orders of magnitude.

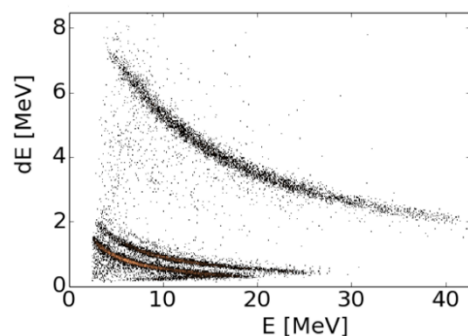


Fig. 2:  $\Delta E$ -E plot of one telescope of the pentagon structure. Protons, deuterons and  $\alpha$ -particles, following the reaction, are nicely separated.

The analysis of the data is in progress. The  $\Delta E$ -E plot,

shown in Fig. 2, displays the statistics from one telescope of the pentagon. The protons, deuterons and  $\alpha$ -particles, following the reaction, are clearly identified. Improvements to the setup and online monitoring are

being implemented, for the continuation of the experiment in 2017 at the XT03 beamline.

## First run with IS562 using HIE-ISOLDE

Results of experiment IS562

*Joakim Cederkäll and Jacob Snäll  
(for the IS562 collaboration)*

The first experiment with HIE-ISOLDE in 2017, using two of the new cryomodules, was carried out in the first part of September by the MINIBALL and IS562 collaborations. The purpose of the IS562 experiment is to use the higher beam energy to expand our earlier investigations of the  $^{100}\text{Sn}$  shell closure, that started at REX-ISOLDE, using multistep Coulomb excitation and transfer reactions.

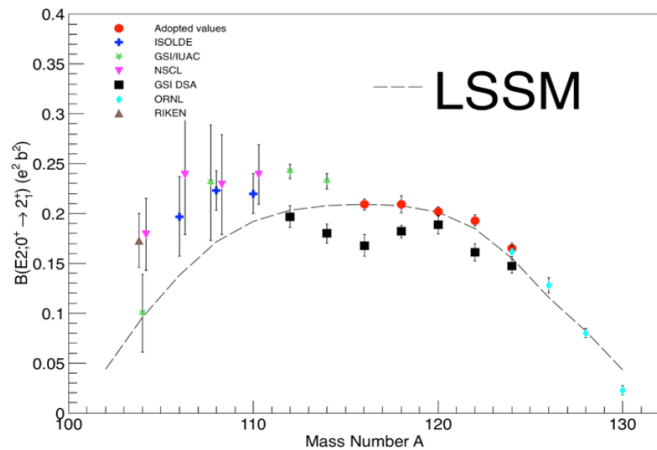


Fig. 1: The trend of measured  $B(E2)$  values in the even Sn isotopes together with results from LSSM calculations.

The results from the previous campaigns at ISOLDE [1, 2], in combination with results from GSI [3], MSU [4] and RIKEN [5] using high-energy Coulomb excitation, showed a clear discrepancy between measurements and predictions from Large Scale Shell Model calculations (LSSM) for the transition probability between the  $0^+$  ground state and the first excited  $2^+$  state in the light even-even Sn isotopes. This result has lent itself to some speculation, and a firm theoretical explanation of the observed deviation has still to be given. LSSM calculations, using standard effective charges for the shell, produce a parabolic trend of the  $B(E2)$  values for the  $0_1^+$  to  $2_1^+$  transition as a function of neutron number, reaching a maximum midshell. This dependence on neutron number, reminiscent of the trend predicted in simple seniority for a single  $j$ -orbit, is however not necessarily a feature for generalized seniority [6]. Above

all, such a trend is now not observed in experiments in the Sn chain (see Fig. 1).

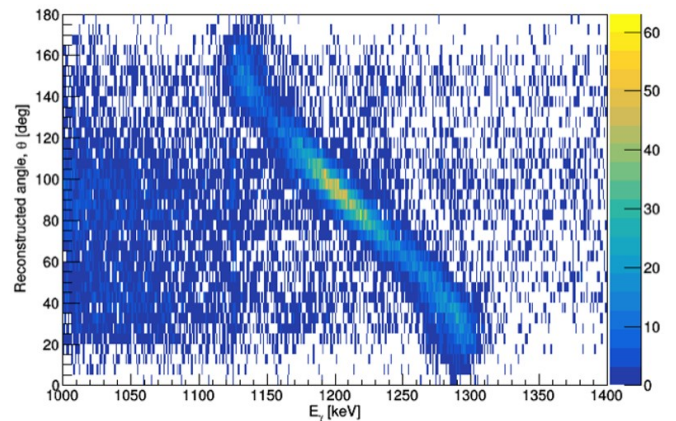


Fig. 2: The detected gamma ray energy for the  $2_1^+ \rightarrow 0_1^+$  transition in  $^{110}\text{Sn}$  plotted against the reconstructed emission angle with respect to the direction of the scattered beam particle (Sn) after detection of the same particle (Sn). Approximately 1/4 of the total statistics is shown.

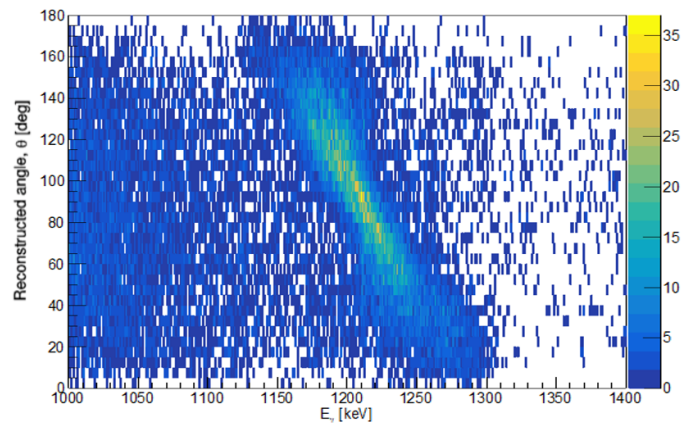


Fig. 3: The same reconstructed emission angle as in Fig. 2 but after detection of the scattered target particle (Pb). The amount of statistics makes it possible to investigate the line shape of the transition in addition to the Coulomb excitation yield (the same amount of the total statistics as in Fig. 2).

The  $B(E2)$  measurements in the unstable light Sn isotopes have until now had rather large statistical errors. With the HIE-ISOLDE configuration used in 2017 energies of up to  $\sim 5$  MeV/u could be reached for beams in this mass region. The increased energy facilitates the use of high-Z targets to increase the statistics from Coulomb excitation events and makes multistep

excitation possible. For the first experiment a beam of  $^{110}\text{Sn}$  at 4.4 MeV/u with an intensity of  $\sim 10^6$  pps was used to bombard a 4 mg/cm<sup>2</sup> target of  $^{206}\text{Pb}$ . Element selection using the RILIS was used before post-acceleration. Measurements of the beam composition showed negligible traces of isobaric contaminants. In total ca 100000 events were collected in the photo peak from the  $2_1^+$  to  $0_1^+$  transition. This result can be compared to the ca 700 events that were collected in the REX-ISOLDE campaign for the same transition. As a result the error of the measurement is now almost completely determined by the precision of the reduced transition probability for the  $2_1^+$  to  $0_1^+$  transition in  $^{206}\text{Pb}$  at ca 3%.

The results for the neutron deficient Sn isotopes have also inspired renewed measurements of the  $B(E2; 0_1^+ \rightarrow 2_1^+)$  values in the stable mid-shell isotopes using different techniques, e.g. line shape analysis. The results from those measurements show statistically

significant deviations from the corresponding adopted values, and also compared to theoretical prediction, i.e. compared to calculations that earlier were in accord with measurements. The high statistics in the  $2^+ \rightarrow 0^+$  transition in the current experiment now opens the door to line shape analysis also in the unstable isotopes (see Figs. 2 and 3). As was mentioned in the introduction, the higher beam energy makes multistep excitation possible. The first  $4^+$  state was also observed in the experiment and a first measurement of its reduced transition probability to the  $2^+$  state will be extracted from the data.

- [1] J. Cederkäll et al., [PRL 98, 172501 \(2007\)](#).
- [2] A. Ekström et al., [PRL 101 012502 \(2008\)](#).
- [3] A. F. Lisetskiy et al., [PRC 70, 044314 \(2004\)](#).
- [4] C. Vaman et al., [PRL 99, 162501 \(2007\)](#).
- [5] P. Doornenbal et al., [PRC 90, 061302\(R\) \(2014\)](#).
- [6] I. O. Morales et al., [PLB 703, 606-608 \(2011\)](#).

## Coulomb excitation of $^{142}\text{Xe}$

Experiment IS548

*C. Henrich*

*(for the MINIBALL collaboration)*

As part of the 2016 campaign with MINIBALL at HIE-ISOLDE the Coulomb excitation measurement with the neutron-rich xenon isotope  $^{142}\text{Xe}$ , the heaviest isotope post-accelerated by HIE-ISOLDE so far, took place. It was a successful experiment with a total beam time of  $\sim 70$  hours.

quadrupole collectivity in this area  $^{142}\text{Xe}$  is a good candidate.

The  $^{142}\text{Xe}$  nuclei were provided by the ISOLDE facility, post-accelerated to 4.5 MeV per nucleon by HIE-ISOLDE and delivered to the MINIBALL experimental area where they impinged on a  $^{206}\text{Pb}$  target with a thickness of 4 mg/cm<sup>2</sup>. The target chamber was surrounded by the MINIBALL detector array with its 24 high purity germanium crystals. As particle detector C-REX, a set of segmented silicon detectors, was used. Fig. 1 shows C-REX during the setup phase in early September 2016. C-REX is an adaptation of T-REX [1] to meet the requirements from Coulomb excitation experiments.

The advantage of the beam energies available at HIE-ISOLDE, compared to REX-ISOLDE, is the increased probability for multi-step processes, important for populating  $4^+$  states and those beyond, as well as single-step excitations of high-lying states, essential to study  $3^-$  states. Figure 2 shows the preliminary gamma-ray spectrum, Doppler corrected with respect to the beam. The comparison to the previous spectrum obtained at REX-ISOLDE (IS411) [2,3] clearly demonstrates the progress from REX- to HIE-ISOLDE enabled by the higher beam energies.

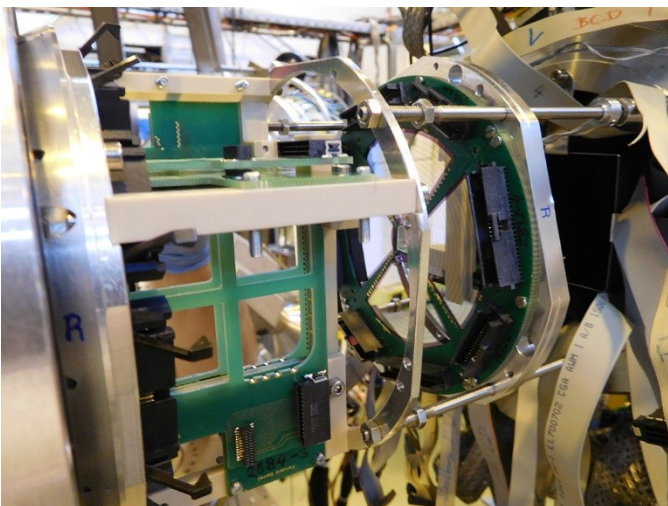


Fig. 1: C-REX particle detector array. Beam direction: Left to right.

$^{142}\text{Xe}$  lies in the vicinity of the doubly magic nucleus  $^{132}\text{Sn}$  and is only two protons below  $^{144}\text{Ba}$ , which exhibits the largest octupole collectivity in the region. To study the onset of octupole collectivity and follow the evolution of

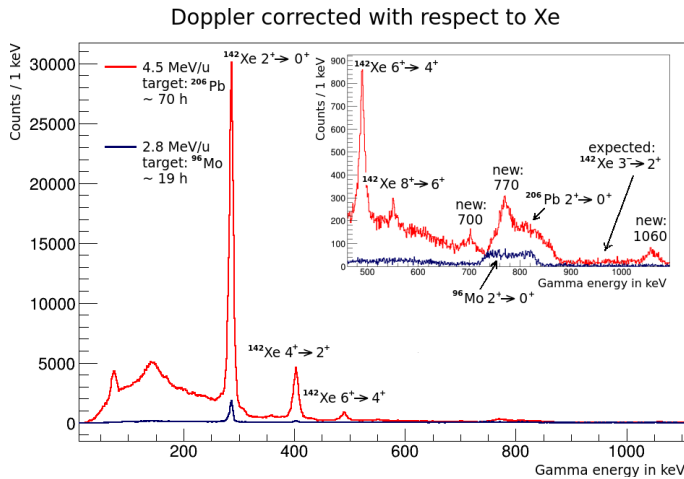


Fig. 2: Red: Preliminary Doppler-corrected gamma-ray spectrum from the HIE-ISOLDE campaign in September 2016. Blue: Comparison to run in 2006 at REX-ISOLDE.

Besides the increase in statistics for the transitions  $2^+ \rightarrow 0^+$  and  $4^+ \rightarrow 2^+$ , which were also seen in the previous

run at REX-ISOLDE, also higher lying transitions, namely  $6^+ \rightarrow 4^+$  and  $8^+ \rightarrow 6^+$ , are visible. The  $3^- \rightarrow 2^+$  transition was expected to have an energy of 971 keV, but it is not visible. However, there are three additional lines in the same energy range in which the missing  $3^- \rightarrow 2^+$  transition was expected which were previously not known.

The ongoing analysis aims to assign these new transitions and clarify the structure of the states based on the reduced transition probabilities and quadrupole moments extracted from the data.

- [1] V. Bildstein et al., [EPJ A 48, 85 \(2012\)](#).
- [2] Th. Behrens, PhD thesis, TU München, 2009.
- [3] C. Henrich, Master thesis, TU Darmstadt, 2014.

## Statistical properties of warm nuclei: the photon strength function of $^{67}\text{Ni}$

Experiment IS559

*V.W. Ingeberg, S.Siem, M.Wiedeking  
(for the IS559 collaboration)*

For a full understanding of the evolution of elemental abundances a wealth of nuclear data is necessary. The production rates depend sensitively on the photon strength function (PSF) and nuclear level density (NLD) due to their central role in nuclear reactions. It has been shown that measured  $(n,\gamma)$  cross section data can be successfully reproduced by using the PSF and NLD data as input for cross section calculations. These cross-sections in turn are inputs for large network calculations of nucleosynthesis in astrophysical environments.

The advantage of using NLDs and PSFs over more traditional approaches to determine capture cross sections lies in its versatility since they can in principle be obtained for any nucleus that can be populated in a reaction from which the excitation energy can be reliably determined. Hence, the measurement of NLDs and PSFs, and therefore  $(n,\gamma)$  cross sections, is not limited to chemically or physically stable isotopes. The full potential of such measurements is unlocked by using inverse kinematics experiments which does not only make available a large range of radioactive species but also previously inaccessible nuclei at stable beam facilities. In 2015, the world's first experiment using inverse kinematic reactions to study the NLD and PSF of  $^{87}\text{Kr}$  was performed at iThemba LABS using the  $d(^{86}\text{Kr},p)^{87}\text{Kr}$  reac-

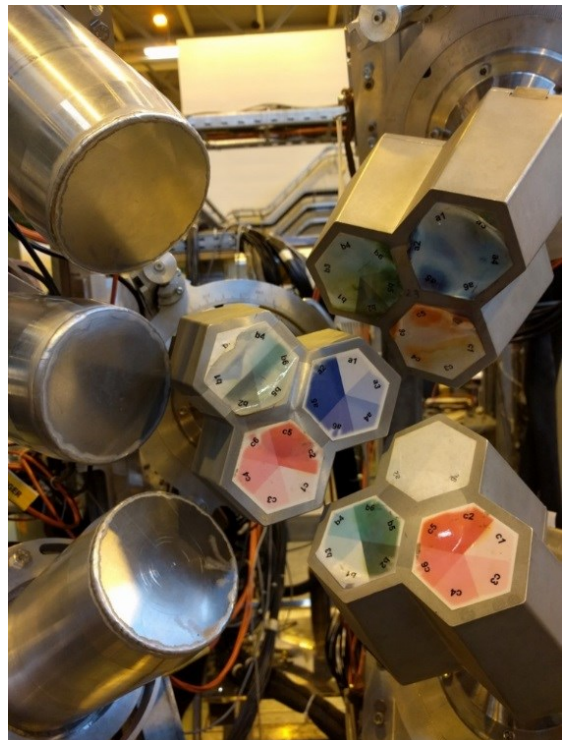


Fig. 1 Six large volume LaBr<sub>3</sub>:Ce detectors were combined with six Miniball HPGe cluster detectors. Shown is half of the sphere, with three of LaBr<sub>3</sub>:Ce detectors to the left and three Miniball clusters to the right.

tion. Effects that are greatly enhanced in inverse kinematics, such as Doppler shift and large angular variations of the fragment energy have been incorporated

into new software developed for the analysis of inverse kinematics experiments. The tremendous success of this proof-of-principle measurement opens up the possibility of measuring the NLD and PSF of nuclei which were previously unavailable for experiments and laid the foundation for the HIE-ISOLDE experiment IS559 which was designed to provide the PSF using two independent methods, the Oslo Method [2] and the Ratio Method [3].

For the experiment the collaboration built upon the success of the first proof-of-principle experiment, and used this same approach to measure the PSF and NLD of  $^{67}\text{Ni}$ . The two methods to extract statistical properties require large amounts of statistics, and six Miniball

cluster detector were combined with six high-efficiency large volume  $\text{LaBr}_3:\text{Ce}$  ( $3.5 \times 8''$ ) detectors. The particle detection was achieved by employing the silicon detectors offered by the C-REX silicon detector setup using CD- and Barrel-detectors. Beam time was received in November 2016. The analyses are in progress and the collaboration is confident that, once available, the results will provide interesting and exciting insight into the PSF and NLD for neutron-rich nuclear systems.

[1] V.W. Ingeberg et al., manuscript in preparation (2017).

[2] A. Schiller et al., [NIM A 447, 498 \(2000\)](#).

[3] M. Wiedeking et al., [PRL 108, 162503 \(2012\)](#).

# Support and contacts

## How to obtain access to the ISOLDE hall

---

1. Use the online pre-registration tool <sup>1</sup> which should be launched by your team leader or deputy team leader. You need to attach the following documents to the pre-registration:
    - a. [Home Institution Declaration](#)<sup>2</sup> signed by your institute's administration (HR).
    - b. Passport
  2. When your pre-registration is accepted by the CERN users office you will receive an email telling you how to activate your CERN computer account.
  3. When you arrive at CERN go to the Users office to complete your registration (Opening hours: 08:30 - 12:30 and 14:00 - 16:00 but closed Wednesday mornings).
  4. Get your CERN access card in [Building 55](#)
- With this registration procedure you become a **CERN user**.
5. Follow the online CERN safety introduction course:
    - a. If you have activated your CERN account, you can access the Safety Awareness course on-line at the web page <http://sir.cern.ch>, from your computer, inside or outside CERN.
    - b. If you have not activated your CERN account, there are some computers available for use without the need to log in on the first floor of building 55 (Your CERN badge will be needed in order to prove your identity).
  6. Complete the following online courses via <https://sir.cern.ch/sir>:
    - a. ISOLDE RP course for Supervised Radiation Areas "Radiation Protection - Supervised Area",
    - b. Electrical Safety - Awareness Course. If you have not activated your CERN account see 5b.
  7. Obtain a Permanent radiation dosimeter at the Dosimetry service, located in [Building 55](#)<sup>3</sup> (Opening hours: Mon. to Fri. 08:30 - 12:00). If you do not need the dosimeter in the following 2 months it should be returned to the Dosimetry service at the end of your visit.  
The "certificate attesting the suitability to work in CERN's radiation areas" <sup>4</sup> signed by your institute will be required.
  8. Follow the 2 hour practical RP safety course and the 2 hour Electrical Awareness Module for which you will have to register in advance<sup>5</sup>. These take place on **Tuesday afternoons** from 13:00 until 17:00 at the training centre (building 6959) in Preveessin. If you do not have your own transport, you can take CERN shuttle 2 from building 500. The timetable for this is [here](#).
  9. Apply for access to "ISOHALL" using ADAMS: <https://www.cern.ch/adams>. This can be done by any member of your collaboration (typically the contact person) having an EDH account<sup>6</sup>. Access to the hall is from the Jura side via your dosimeter.
- Find more details about CERN User registration see the [Users Office website](#). For the latest updates on how to access the ISOLDE Hall see the [ISOLDE website](#).
- New users are also requested to visit the ISOLDE User Support office while at CERN.
- Opening hours:  
Monday to Friday 08:30-12:30

<sup>1</sup> For information see <http://usersoffice.web.cern.ch/new-registration>

<sup>2</sup> The Home Institute Declaration should not be signed by the person nominated as your team leader.

<sup>3</sup> <http://cern.ch/service-rp-dosimetry> (open *only in the mornings* 08:30 - 12:00).

<sup>4</sup> The certificate can be found via <http://isolde.web.cern.ch/get-access-isolde-facility>

<sup>5</sup> For Information about how to register see

<http://isolde.web.cern.ch/get-access-isolde-facility>

<sup>6</sup> Eventually you can contact Jenny or the Physics coordinator.



## Contact information

---

### ISOLDE User Support

Jenny Weterings

[Jennifer.Weterings@cern.ch](mailto:Jennifer.Weterings@cern.ch)

+41 22 767 5828

### Chair of the ISCC

Bertram Blank

[blank@cenbg.in2p3.fr](mailto:blank@cenbg.in2p3.fr)

+33 5 57 12 08 51

### Chair of the INTC

Karsten Riisager

[kvr@phys.au.dk](mailto:kvr@phys.au.dk)

+45 87 15 56 24

### ISOLDE Physics Section Leader

Maria J.G. Borge

[mgb@cern.ch](mailto:mgb@cern.ch)

+41 22 767 5825

### ISOLDE Physics Coordinator

Karl Johnston

[Karl.Johnston@cern.ch](mailto:Karl.Johnston@cern.ch)

+41 22 767 3809

### ISOLDE Technical Coordinator

Richard Catherall

[Richard.Catherall@cern.ch](mailto:Richard.Catherall@cern.ch)

+41 22 767 1741

### HIE-ISOLDE Project Leader

Yacine Kadi

[Yacine.Kadi@cern.ch](mailto:Yacine.Kadi@cern.ch)

+41 22 767 9569

More contact information at

<http://isolde.web.cern.ch/contacts/isolde-contacts> and at  
<http://isolde.web.cern.ch/contacts/people>